# White Paper on

# Seismic Hazard in the Eastern Tennessee Seismic Zone

Prepared for

Electric Power Research Institute

By

Risk Engineering, Inc.

Boulder, Colorado

May 12, 2008

## TABLE OF CONTENTS

## INTRODUCTION

This study examines the seismic hazard at a site located in the Eastern Tennessee Seismic Zone (ETSZ) and examines the sensitivity of hazard at that site to different assumptions on seismicity in the region. As background, the Electric Power Research Institute (EPRI, 1989) conducted a large study of seismic hazard in the central and eastern US (CEUS) in the 1980s—known as the EPRI-SOG study since it was funded by the Seismicity Owners Group—that has become the starting point for recent assessments of seismic hazard for current nuclear plant license applications. Several updates of the EPRI-SOG study have been made in recent license applications to account for new information, particularly for the New Madrid seismic zone and for the Charleston, South Carolina regions, both of which have experienced large earthquakes in historical times.

The ETSZ has been included in two additional studies, the first a study conducted by Lawrence Livermore National Laboratory (LLNL, 2002) herein termed the "TIP study" (it was designated the Trial Implementation Project), and the second a study conducted by Geomatrix (2004) herein termed the "DSS study" (it was designated the TVA Dam Safety Study). The 6 Earth Science Teams that participated in the original EPRI-SOG study identified the ETSZ as a possible source of earthquakes, with varying credibility ascribed to a local source representing that seismicity. Over all the various EPRI-SOG interpretations, the maximum magnitude possible for the ETSZ was given a wide distribution that, on the moment magnitude scale **M**, represented values of $\mathbf{M}_{max}$ from 4.5 to 7.5, with a mean value of about 6.0 (see Figure 1, taken from Ref. 3). The TIP and DSS studies developed their own evaluations of the ETSZ and also assigned a broad range of maximum magnitudes to this zone, from $\mathbf{M}_{max}$ 5.25 to 8.25 (see Figure 1). The mean $\mathbf{M}_{max}$ value for both the TIP and DSS studies is about 6.6.

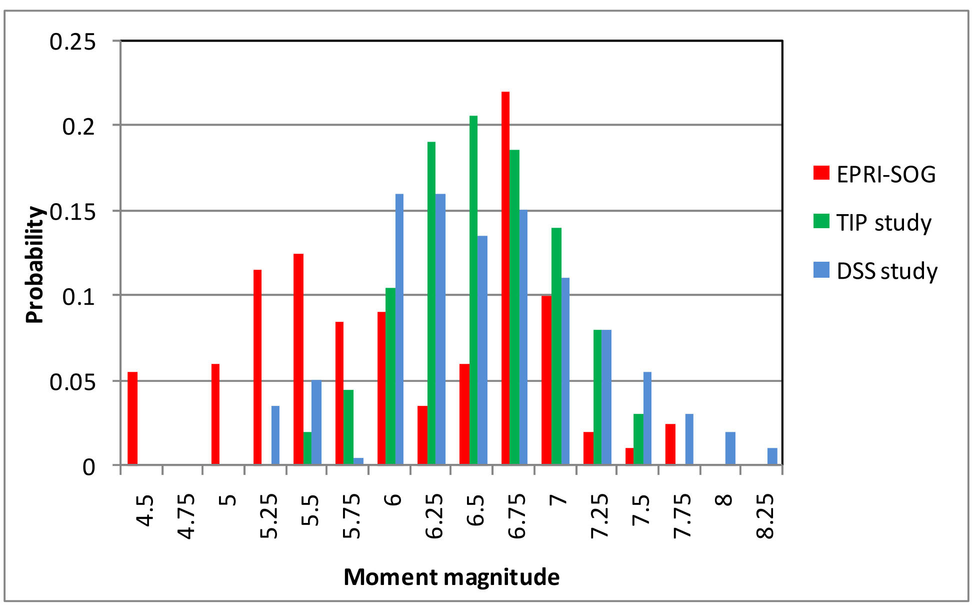


**Figure 1: $m_{max}$ distribution (in terms of M scale) for ETSZ, derived from Ref. 3.**

.

The largest historical earthquake recorded in the ETSZ is less than 5.0, and no evidence of large paleo-earthquakes has been documented in the ETSZ, so values of $\mathbf{M}_{max}$ must be inferred from geology, tectonics, and analogies with other regions throughout the world. Such inferences are subject to large uncertainties, resulting in the broad range of values shown in Figure 1.

In order to determine the effect of alternative interpretations of $\mathbf{M}_{max}$ for the ETSZ on seismic hazard from the EPRI-SOG study, one must examine and evaluate how the EPRI-SOG study should be updated to account for new information. For example, the alternative $\mathbf{M}_{max}$ values for the ETSZ might themselves be very influential on seismic hazard at a site close to or within the ETSZ, but if the total hazard at that site is dominated by some other source and the ETSZ contributes a small fraction of the total hazard, changes caused by alternative $\mathbf{M}_{max}$ values would have a minor effect. Also, the EPRI-SOG study was a multi-million dollar, multi-year effort involving 20-25 earth scientists evaluating earthquake sources, and the resulting interpretations should not be completely discarded in favor of alternative interpretations that do not necessarily represent a consensus of scientific opinion.

With this perspective, updating the ETSZ interpretations must also include updating the catalog of seismicity in the CEUS since the EPRI-SOG study. The EPRI-SOG catalog of earthquakes included events through 1984, and most comparisons of seismicity rates indicate that, if anything, mean seismicity rates in the ensuing 23+ years have decreased.

Thus the overall path followed by this study has the following tasks:

<u>Task 1: Update seismicity catalog.</u> Several regional catalogs are used to extend the EPRI-SOG catalog from 1984 to 2006, the most recent year for which complete data are available.

<u>Task 2: Modify seismicity rates and $m_{max}$ values of EPRI-SOG teams.</u> The seismicity parameters and $m_{max}$ values of seismic sources used to represent the ETSZ are modified to reflect the updated seismicity catalog and to parallel the interpretations of maximum magnitudes used in the TIP and DSS studies.

<u>Task 3: Determine sensitivity to alternative interpretations.</u> The seismic hazard using the modified parameters is compared to the hazard with the original EPRI-SOG parameters to quantify the effect of any change in seismic hazard on ground motions that might be used for seismic design.

<u>Task 4: Perform integration using alternative interpretations and determine significance.</u> If the sensitivity from Task 3 indicates that the alternative assumptions are potentially significant, determine how the alternative assumptions might be incorporated into a seismic hazard analysis in a balanced way. As stated above, it would not be appropriate to completely discard the

interpretations of a major, multi-year study to adopt alternative assumptions that are not based on new data or on widely accepted scientific interpretation. Once the alternative assumptions are incorporated in a balanced way, determine the impact on seismic hazard and evaluate whether the alternative assumptions are significant.

The remainder of this report describes the application of these tasks to the ETSZ and the conclusions regarding seismic hazard.

## UPDATED SEISMICITY CATALOG

The region in the CEUS that was examined for updated seismicity is shown in Figure 2. This region was selected because it encompasses all seismic sources used to depict the ETSZ for the 6 EPRI-SOG teams (see the next section). Updating the seismicity parameters for these sources requires an updated earthquake catalog for the entire region covered by any of these seismic sources.

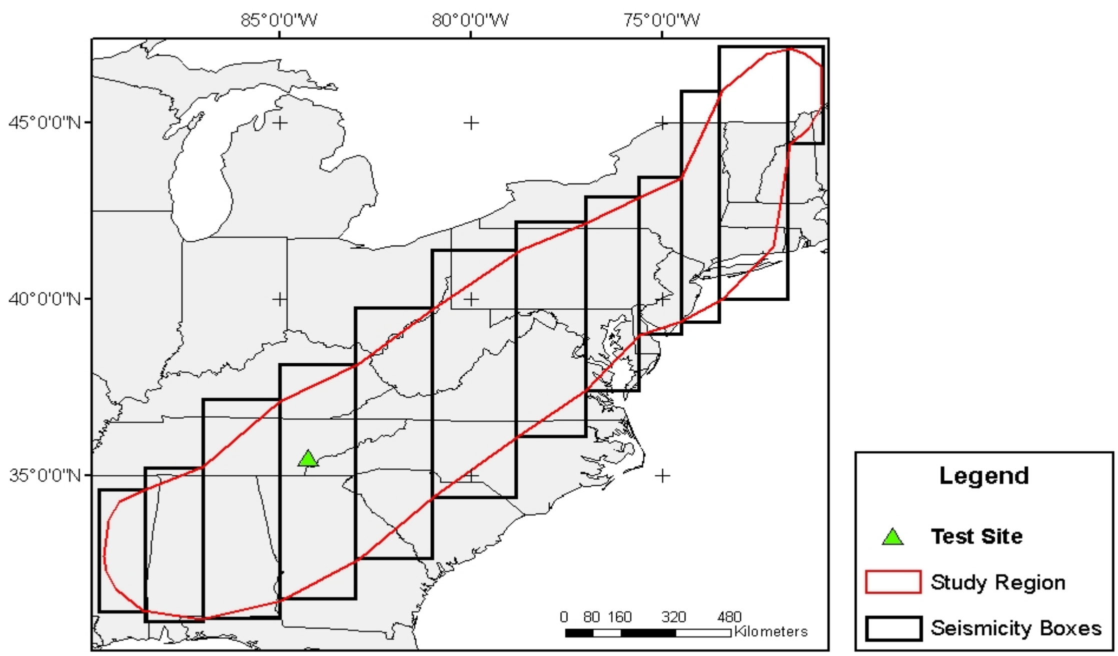


**Figure 2. Study region for updated earthquake catalog (shown in red), and longitude-latitude boxes used to collect earthquakes for analysis.**

Four regional earthquake catalogs were compiled to develop a composite catalog for the entire region shown in Figure 2. In all cases, earthquakes with $m_b \geq 3$ in the study region were used. These four catalog sources were:

Southeastern US Seismic Network. The Virginia Tech Seismological Observatory (VTSO) compiles the Southeastern US Seismic Network (SEUSN) Bulletins, which contain earthquakes from 1977 through 2005. These bulletins are available from the VTSO website. An additional file contains earthquakes in 2006. Non-seismic events (mine blasts, explosions) have been removed from these catalogs. Figure 3 shows the region where the SEUSN is considered "authoritative" by the Advanced National Seismic System (ANSS).

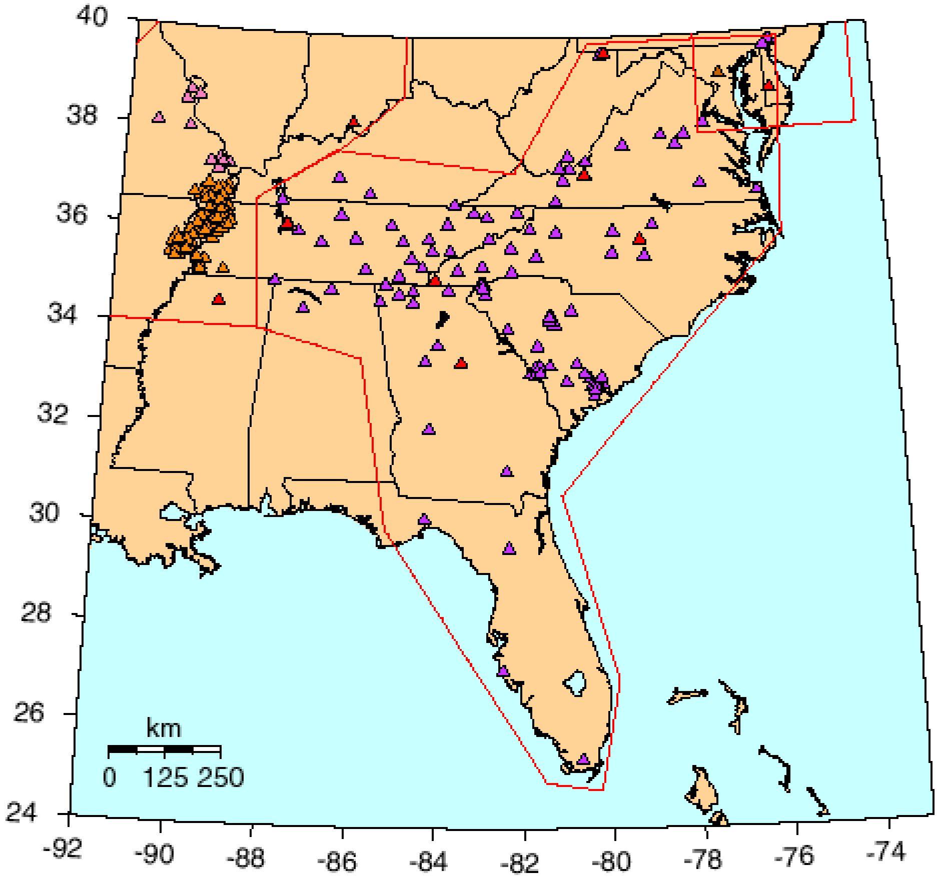


**Figure 3. Region where SEUSN is considered authoritative by ANSS (from ANSS website). Blue triangles are SEUSN seismic stations, other triangles are stations run by other networks.**

Lamont-Doherty Cooperative Seismographic Network. The Lamont-Doherty Earth Observatory, part of Columbia University, operates the Lamont-Doherty Cooperative Seismographic Network (LCSN). The LCSN catalog can be downloaded from the LCSN website, giving earthquakes from 1970 to present. Earthquakes from 1985—2006 were used in the current study. Figure 4 shows the region where the LCSN is considered “authoritative” by the Advanced National Seismic System (ANSS).

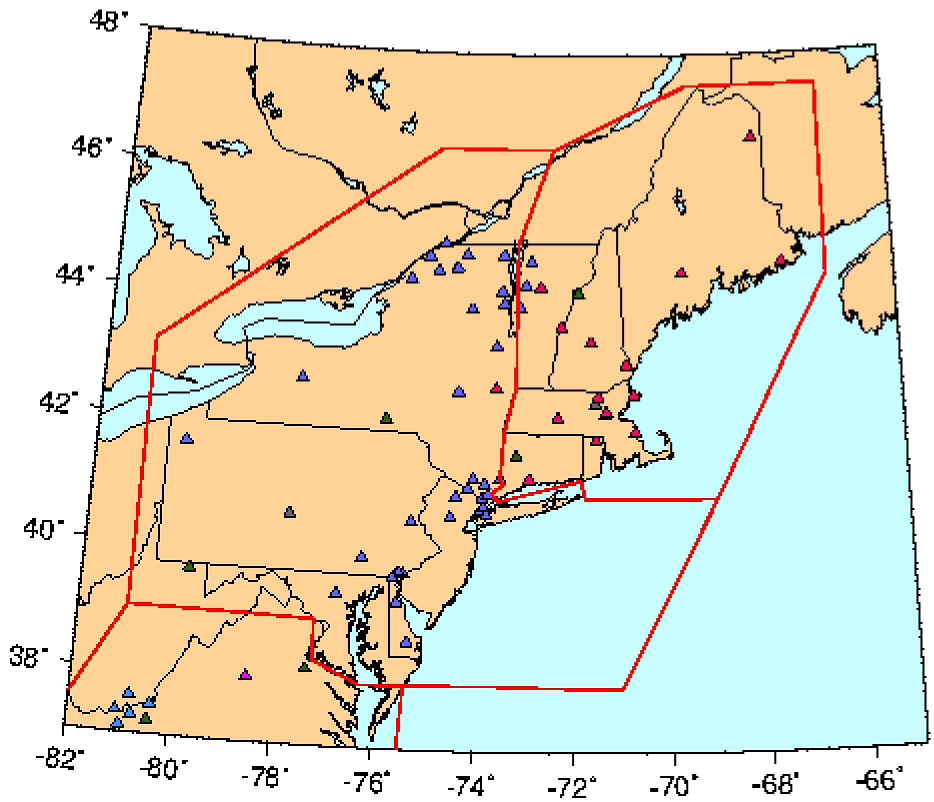


**Figure 4: Regions for which LCSN (in New York, Pennsylvania, and adjacent states) and NESN (in New England) are considered authoritative by ANSS (from ANSS website). Blue triangles are LCSN seismic stations, red triangles are NESN seismic stations, other triangles are stations run by other networks.**

New England Seismic Network. The New England Seismic Network (NESN) is operated by Weston Observatory, part of Boston College. Weston Observatory publishes quarterly bulletins for the NESN data, which are available from the Weston Observatory website. Separate catalogs are available for the years 1568-1990, 1990-1999, and 2000-2005. Quarterly bulletins are available to augment the catalog for 2006. Note that the first 2 catalogs overlap for the year 1990, and the locations and magnitudes contained in the 1st catalog for the year 1990 are preferred.

National Earthquake Information Center. The US Geological Survey/National Earthquake Information Center (NEIC) publishes a monthly Preliminary Determinations of Epicenters (PDE) listing. This list is the most complete computation of hypocenters and magnitudes done by the USGS NEIC. It is normally produced a few months after the events occur. The publication is called “Preliminary” because the “final” computation of hypocenters for the world is considered to be the Bulletin of the International Seismological Centre (ISC), which is produced about two years after the earthquakes occur. NEIC is considered the default authoritative source for earthquakes outside the local network regions shown in Figures 3 and 4. The NEIC catalog was used to supplement the other 3 catalogs in central and southern Alabama, and in eastern Kentucky and western West Virginia.

Earthquakes with $m_b \geq 3$ in the four catalogs were assembled, duplicates and dependent events (foreshocks and aftershocks) were removed with preference on duplicate events going to the seismic network considered to be authoritative by ANSS (as shown in Figures 3 and 4). The only exception was that in central and southern Alabama, the locations and magnitudes of the SEUSN were adopted over those of the NEIC catalog, based on the advice of network operators (Chapman, personal communication, 2008). To identify duplicates and dependent events, the algorithm of Gardner and Knopoff (1974) was used as a flag, and all flagged events were individually examined. The result was a catalog of 136 earthquakes in the study region from 1985-2006 with $m_b \geq 3$ that can be used to extend the EPRI catalog. Figure 5 shows earthquakes from the original EPRI-SOG catalog and the additional 136 earthquakes identified in the study region. Figure 5 also shows the location of the test site used for seismic hazard calculations described below.

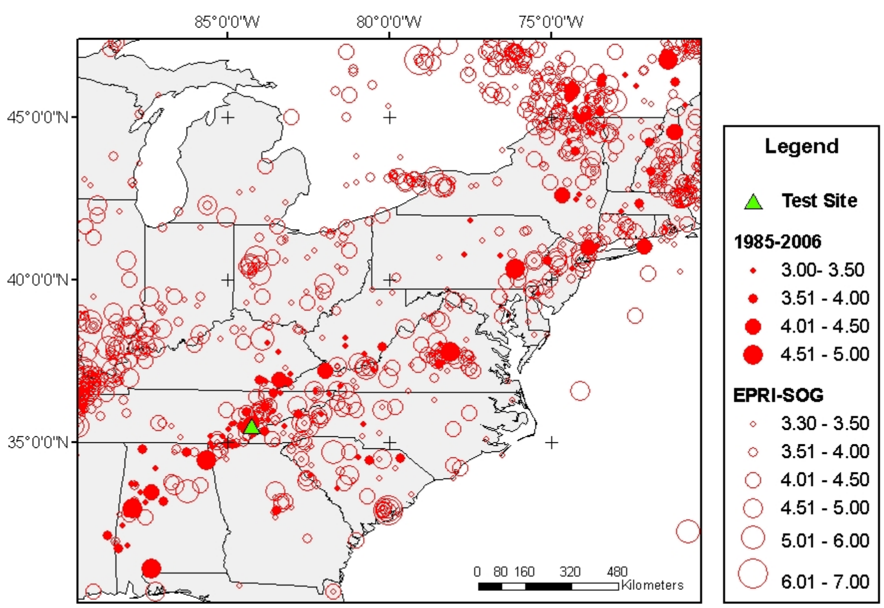


**Figure 5: Original EPRI-SOG earthquakes, and earthquakes in the extended catalog.**

## MODIFICATION OF SEISMICITY RATES AND $\mathbf{M}_{max}$ VALUES.

The EPRI-SOG team sources representing seismicity in the region of the ETSZ were updated to calculate revised seismicity parameters using the extended earthquake catalog. These updated sources are listed in Table 1 with their probabilities of activity ($P_a$).

**Table 1. EPRI-SOG team sources representing the ETSZ and related background zones.**

| Team | Source | Name | $P_a$ | Comment |
|---|---|---|---|---|
| Bechtel | BEC-24 | Bristol trends | 0.25 | ETSZ source |
| | BEC-25 | NY-AL lineament | 0.30 | ETSZ source |
| | BEC-25A | Altern. for 25 | 0.45 | ETSZ source |
| Dames & Moore | DAM-04 | Appalachian fold belt | 0.35 | ETSZ source |
| | DAM-4A | Kink in fold belt | 0.65 | ETSZ source |
| Law Engineering | LAW-17 | Eastern basement | 0.62 | ETSZ source |
| | LAW-217 | Background for 17 | 0.38 | Background |
| Rondout | RND-13 | So. NY-AL lineament | 1.0* | Adjacent source |
| | RND-25 | So. Appalachians | 0.99* | ETSZ source |
| | RND-27 | TN-VA border zone | 0.99* | Adjacent source |
| Woodward-Clyde | WCC-31 | Blue Ridge comb. | 0.024 | ETSZ source |
| | WCC-31A | Blue Ridge comb.—Altern. | 0.211 | ETSZ source |
| | WCC-BG | Background | 0.765 | Background |
| Weston | WGC-24 | NY-AL Clingman | 0.90 | ETSZ source |
| | WGC-103 | So. Appal. background | 0.10 | Background |

*-- Rondout source RND-25 overlays most of the ETSZ, see Figure 9. $P_a$ was taken as 1.0 for all three sources. The two adjacent sources were treated conservatively here as though they also represent the ETSZ.

Maps of each team's seismic sources listed in Table 1 are shown in Figures 6-11. Note that the notch in Figure 7 for Dames & Moore sources 4 and 4A is covered by source DAM-05, which is not modeled here. Note also that many EPRI-SOG sources extend well outside the ETSZ, and increasing $\mathbf{M}_{max}$ values in those areas would produce conservative estimates of seismic hazard that are not justified by the TIP and DSS studies. Also, many EPRI-SOG teams sources adjacent to the ETSZ have not been modeled here, because the focus is on the ETSZ, and therefore the sets of sources shown in Figures 6-11 would not be appropriate for a site located outside the ETSZ.

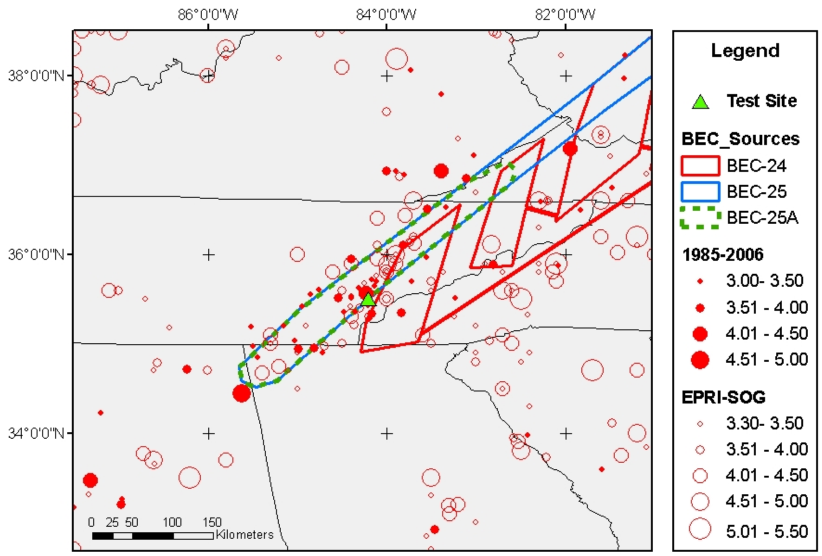


**Figure 6: Map of Bechtel team seismic sources and historical seismicity.**

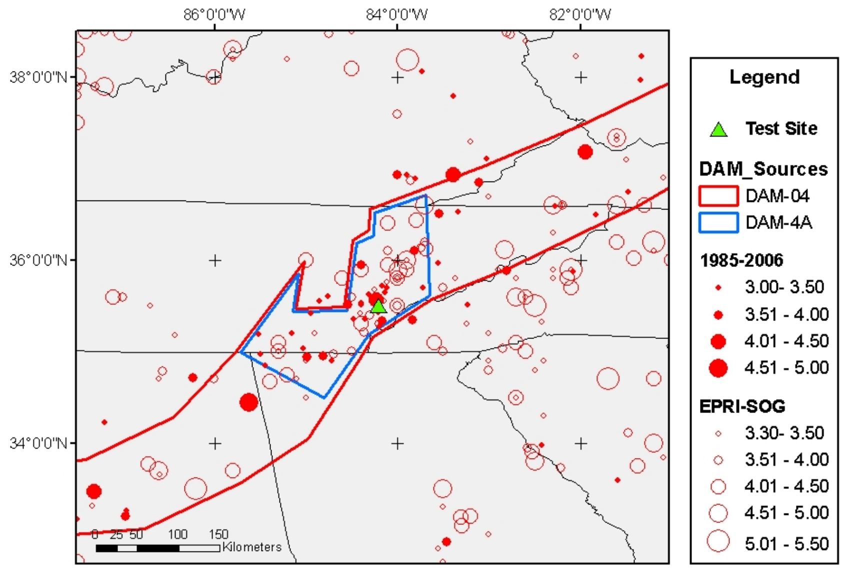


**Figure 7: Map of Dames & Moore team seismic sources and historical seismicity.**

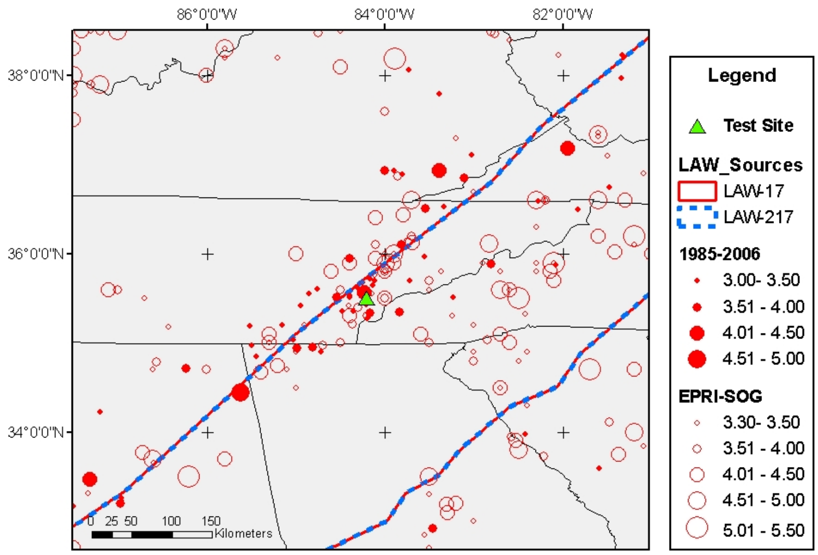


**Figure 8: Map of Law team seismic sources and historical seismicity.**

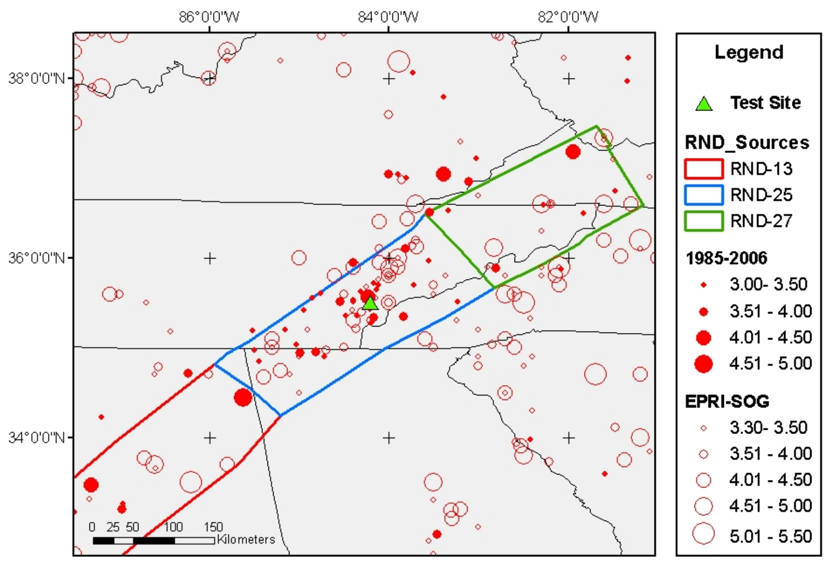


**Figure 9: Map of Rondout team seismic sources and historical seismicity.**

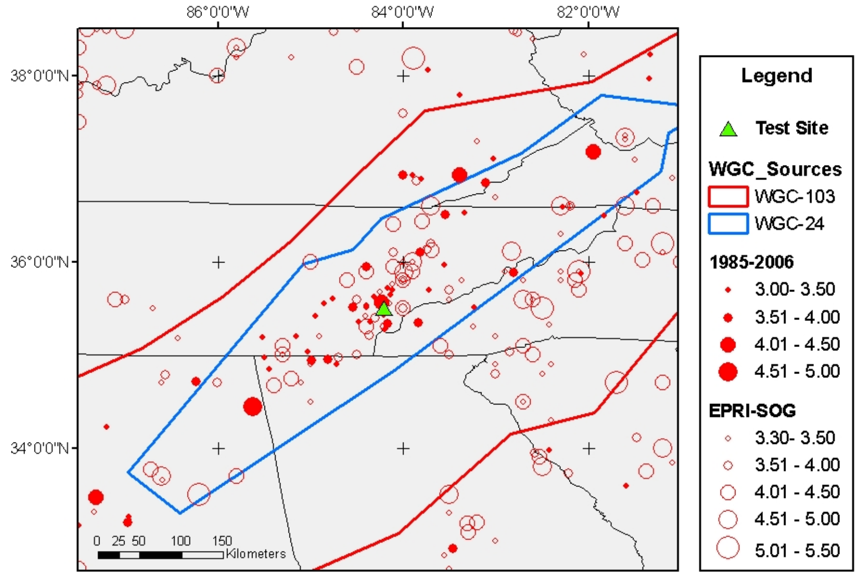


**Figure 10: Map of Weston team seismic sources and historical seismicity.**

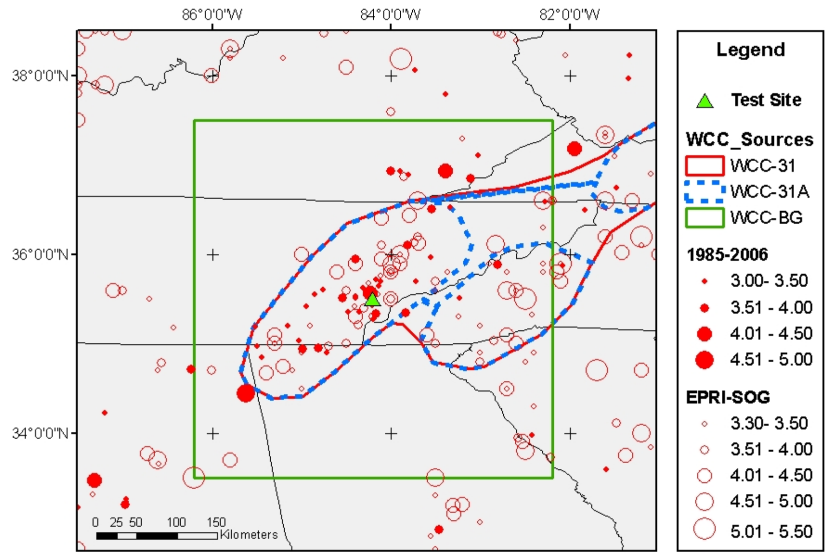


**Figure 11: Map of Woodward-Clyde team seismic sources and historical seismicity.**

Smoothing assumptions on seismicity parameters for all sources are summarized in Ref. 5, and these smoothing assumptions were used with the EPRI-SOG computer program EQPARAM to calculate updated seismicity parameters using the extended catalog.

Maximum magnitude values were updated using the probability mass functions shown in Figure 1, which are reproduced in Figure 12 for just the TIP and DSS studies. The values in Figure 12 are in terms of moment magnitude **M**, and the seismicity of the EPRI-SOG sources is described by body-wave magnitude $m_b$, so a conversion was necessary between the two scales. Three published conversion equations were used for this purpose: Atkinson and Boore (1995), EPRI (1993), and Frankel et al (1996). These conversion equations are reasonably consistent for **M** between 4.5 and 8, as shown in Figure 13, and an equally weighted average of the 3 equations was used for magnitude conversion.

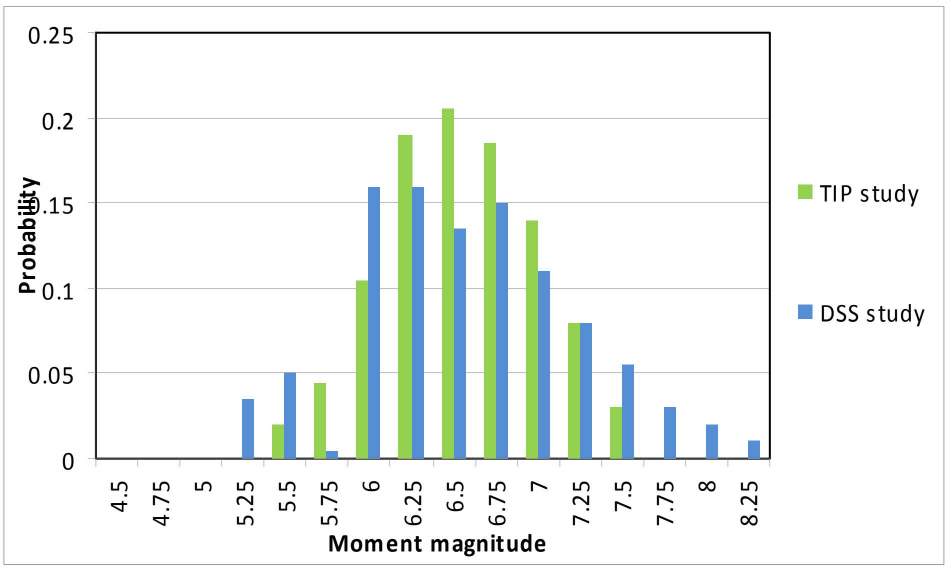


**Figure 12: Reproduction of TIP and DSS distributions from Figure 1.**

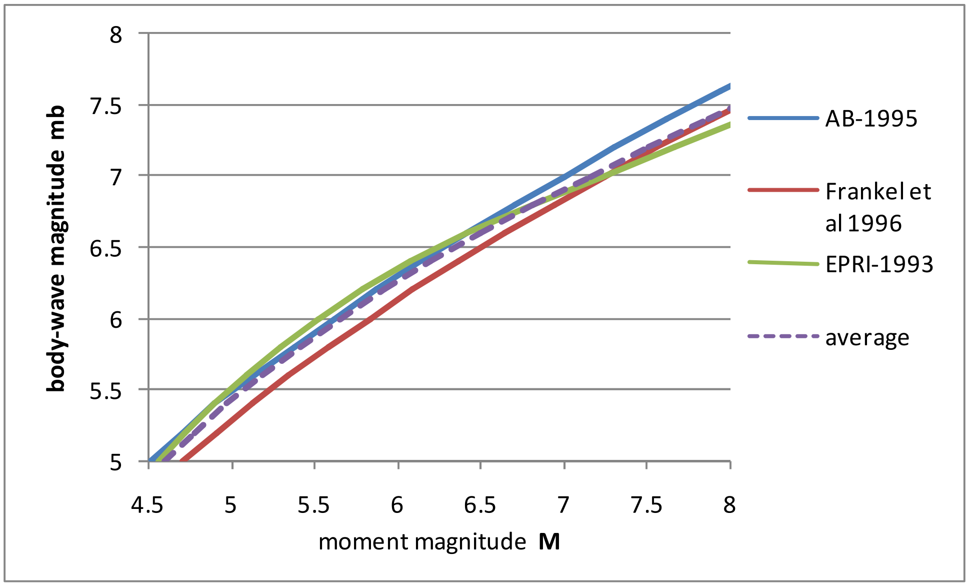


**Figure 13: Conversion equations between M and $m_b$.**

Values used to represent the **M** distribution in Figure 12 are shown in Table 2, along with equivalent $m_b$ distributions and "chosen $m_b$ values" which were selected at even 0.1 magnitude increments to be consistent with numerical integrations in seismic hazard calculations. Three magnitude values were selected using the mean and mean $\pm 1.4\times\sigma$ values of the original **M** distribution, and these 3 values were weighted 0.28, 0.44, 0.28. These values and weights accurately replicated the mean and σ values of the original distributions. These 3-point distributions were developed for the TIP study, the DSS study, and a composite distribution of the two.

**Table 2. Magnitude distributions for TIP study, DSS study, and composite distribution.**

| Distribution | | Lower (wt=0.28) | Central (wt=0.44) | Upper (wt=0.28) | mean | σ |
|---|---|---|---|---|---|---|
| TIP | **M** value | 6.27 | 6.55 | 6.83 | 6.55* | 0.21* |
| | equiv. $m_b$ value | 6.45 | 6.64 | 6.80 | 6.63 | 0.13 |
| | chosen $m_b$ value | 6.4 | 6.6 | 6.8 | 6.6 | 0.15 |
| DSS | **M** value | 6.01 | 6.58 | 7.15 | 6.58* | 0.43* |
| | equiv. $m_b$ value | 6.26 | 6.67 | 7.00 | 6.64 | 0.28 |
| | chosen $m_b$ value | 6.2 | 6.6 | 7.0 | 6.6 | 0.30 |
| Composite | **M** value | 6.13 | 6.56 | 6.99 | 6.56* | 0.32* |
| | equiv. $m_b$ value | 6.35 | 6.64 | 6.91 | 6.63 | 0.21 |
| | chosen $m_b$ value | 6.3 | 6.6 | 6.9 | 6.60 | 0.22 |

*--values consistent with distribution from Figure 12.

The TIP and DSS studies are consistent in terms of mean $\mathbf{M}_{max}$ value, with both studies indicating a mean $\mathbf{M}_{max}$ of about 6.6. The TIP study has a smaller σ of 0.21 compared to 0.43 for the DSS study, and the composite distribution indicates a σ of 0.32. The σ values for the distributions in terms of $m_b$ are somewhat lower because the slope of the **M-to-**$m_b$ conversion is less than 1 (Figure 13).

**SENSITIVITY TO ALTERNATIVE INTERPRETATIONS**

To examine the effects of the extended catalog and the alternative $m_{max}$ distributions, a test site was chosen at location 84.2°W, 35.5°N (see Figure 14). This site lies near the center of historical seismicity in the region and is a representative test case in the sense that any increase in hazard caused by the alternative $m_{max}$ distribution will affect this site directly, compared to a site at the edges of the ETSZ or farther away where the ETSZ will have relatively less contribution to total seismic hazard. Note that the geometry of the ETSZ depends on the study and the specific interpretation.

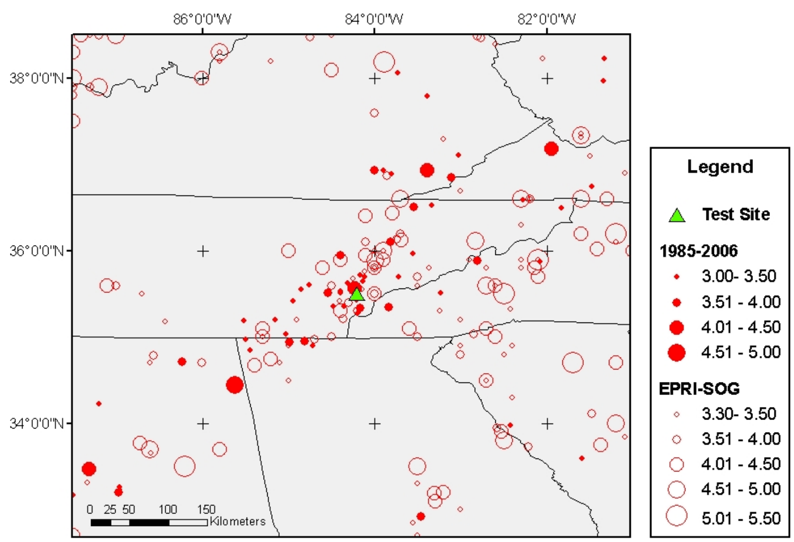


**Figure 14. Map showing seismicity in ETSZ region from EPRI-SOG catalog, from extended catalog (1985—2006), and showing location of test site.**

In order to properly represent the seismic hazard at the test site, several additional sources were included in the hazard calculations. These were the New Madrid faults, which were represented using the model developed for the Clinton ESP application (Exelon, 2003), and the Charleston seismic zone, which was represented using the model developed for the Vogtle ESP application (Ref. 10). These sources had the following characteristic magnitude ranges:

| | Characteristic magnitudes |
|---|---|
| New Madrid faults | 7.0—7.9 |
| Charleston seismic zone | 6.7—7.5 |

Three New Madrid faults are included in the model: the Blytheville fault, the East Prairie fault, and the Reelfoot fault. Earthquake occurrences were represented with a cluster model, accounting for the likelihood that a large earthquake on one fault will trigger large earthquakes on the other 2 faults (as happened in 1811-1812), and the parameters for the cluster model were taken from Ref. 3.

The test site shown in Figure 14 will accentuate any effect of an alternative $m_{max}$ distribution for the ETSZ because only seismic sources representing the ETSZ, the New Madrid faults, and the Charleston seismic zone will be modeled. In a typical seismic hazard, adjacent seismic sources also contribute to seismic hazard, thus diluting the influence of any one source, but these adjacent seismic sources are not modeled here, for the sake of simplicity. As noted above, the test site is located near the center of the ETSZ and is within the seismic sources used to characterize the ETSZ by the EPRI-SOG teams.

Seismic hazard was calculated with the EPRI (2004) ground motion equations, using the Abrahamson and Bommer (2006) updated standard deviations representing aleatory uncertainty for those equations. These equations and aleatory uncertainties are available for spectral acceleration at 7 spectra frequencies: 100 Hz, 25 Hz, 10 Hz, 5 Hz, 2.5 Hz, 1 Hz, and 0.5 Hz. Hazard calculations were made, both without and with the Cumulative Absolute Velocity (CAV) filter documented by Hardy et al (2006) for both the original EPRI-SOG parameters and the alternative parameters. All calculations were made for hard-rock site conditions.

Seismic hazard was first calculated with the original EPRI-SOG seismicity parameters and $m_{max}$ distributions for the ETSZ and with the updated New Madrid faults and Charleston seismic zone. This calculation used the source representation for the ETSZ indicated in Table 1. Specifically, the Bechtel team had 3 alternative representations for the ETSZ, with the $P_a$ values shown in Table 1. Dames & Moore had 2 alternative representations. Law Engineering had one interpretation with $P_a$ of 0.62, with a background active (with the complementation probability of 0.38) when the ETSZ was not active. The Rondout team had 3 sources, with $P_a$=1, representing parts of the ETSZ. Woodward-Clyde had 2 alternative representations, with a background zone active when neither of the ETSZ representations was active. Weston had one ETSZ and a background zone.

Plots of mean seismic hazard by source for each team for the non-CAV hazard calculation are included in Appendix A for 10 Hz and 1 Hz, those being typical measures of high- and low-frequency seismic hazard. Generally the ETSZ and background zones dominate the hazard for high frequencies, but the New Madrid faults show an important contribution at 1 Hz. The Charleston seismic zone generally does not contribute significantly to hazard.

A second calculation of seismic hazard was made with alternative parameters (updated seismicity parameters and the alternative $m_{max}$ distribution summarized in Table 2). For this (and subsequent) calculations, the "composite distribution" of Table 2 was used. This alternative $m_{max}$ distribution was applied to all ETSZ sources listed in Table 1, but not to background zones since these represent the interpretation (and probability) that a separate ETSZ does not exist.

Table 3 compares the $10^{-4}$ and $10^{-5}$ UHRS amplitudes and the GMRS amplitudes for the two calculations. The GMRS is calculated per Reg. Guide 1.208 using the following equations:

$$A_R = SA(10^{-5)}/ SA(10^{-4)} \quad (1)$$

$$GMRS = \max[SA(10^{-4})\times\max(1.0, 0.6\ A_R^{0.8}), 0.45 \times SA(10^{-5)}] \quad (2)$$

where $SA(10^{-4})$ is the spectral acceleration for the $10^{-4}$ UHRS, and similarly for $SA(10^{-5})$. Table 4 shows a similar comparison that is identical in all respects except that this comparison is made between the original, CAV-filtered hazard and the alternative assumptions using the CAV-filtered hazard.

**Table 3: Comparison between GMRS at test site for original EPRI-SOG parameters and alternative parameters, non-CAV hazard (note: % differences were calculated with more decimal places than are shown in the tables).**

| Freq. (Hz) | Orig 1E-4 (g) | Orig 1E-5 (g) | GMRS (g) | Alt. 1E-4 (g) | Alt. 1E-5 (g) | GMRS (g) | % DIFF |
|---|---|---|---|---|---|---|---|
| 100 | 0.264 | 0.875 | 0.413 | 0.280 | 0.915 | 0.433 | 4.9% |
| 25 | 0.725 | 2.45 | 1.15 | 0.765 | 2.56 | 1.21 | 4.8% |
| 10 | 0.480 | 1.48 | 0.709 | 0.508 | 1.548 | 0.743 | 4.9% |
| 5 | 0.306 | 0.896 | 0.434 | 0.322 | 0.942 | 0.456 | 5.2% |
| 2.5 | 0.173 | 0.454 | 0.225 | 0.180 | 0.475 | 0.235 | 4.6% |
| 1 | 0.0894 | 0.217 | 0.109 | 0.0911 | 0.220 | 0.111 | 1.4% |
| 0.5 | 0.0615 | 0.165 | 0.0814 | 0.0620 | 0.165 | 0.0814 | 0.0% |

**Table 4: Comparison between GMRS at test site for EPRI-SOG parameters and alternative parameters, CAV-filtered hazard (note: % differences were calculated with more decimal places than are shown in the tables).**

| Freq. (Hz) | Orig 1E-4 (g) | Orig 1E-5 (g) | GMRS (g) | Alt. 1E-4 (g) | Alt. 1E-5 (g) | GMRS (g) | % DIFF |
|---|---|---|---|---|---|---|---|
| 100 | 0.135 | 0.885 | 0.398 | 0.157 | 0.929 | 0.418 | 5.0% |
| 25 | 0.351 | 2.43 | 1.09 | 0.410 | 2.56 | 1.15 | 5.4% |
| 10 | 0.257 | 1.43 | 0.644 | 0.295 | 1.51 | 0.681 | 5.8% |
| 5 | 0.191 | 0.842 | 0.379 | 0.210 | 0.893 | 0.402 | 6.1% |
| 2.5 | 0.114 | 0.422 | 0.195 | 0.122 | 0.445 | 0.206 | 5.8% |
| 1 | 0.0545 | 0.202 | 0.0933 | 0.0572 | 0.205 | 0.0954 | 2.2% |
| 0.5 | 0.0302 | 0.149 | 0.0672 | 0.0314 | 0.149 | 0.0671 | -0.2% |

Tables 3 and 4 show that, for a site located near the center of seismicity in the ETSZ, when surrounding sources are not included in the analysis, and when all ETSZ of the EPRI-SOG teams are modified to adopt the alternative $m_{max}$ distribution, the potential change in GMRS is about 6% or less, across all spectral frequencies. Figure 15A plots the PGA hazard curves for the original parameters and for the alternative parameters. Figure 15B expands Figure 15A for PGA amplitudes between 0.1g and 1g, and for annual frequencies between $10^{-4}$ and $10^{-5}$. The small triangle in Figure 15B illustrates the effect of the 5% change in the GMRS from Table 4 (from 0.418g to 0.398g). Decreasing the GMRS by 5% will, for these amplitudes, imply a 6% increase in annual frequency of exceedence, because the log-log slope of the hazard curve is almost -1 (due to the effect of the CAV filter).

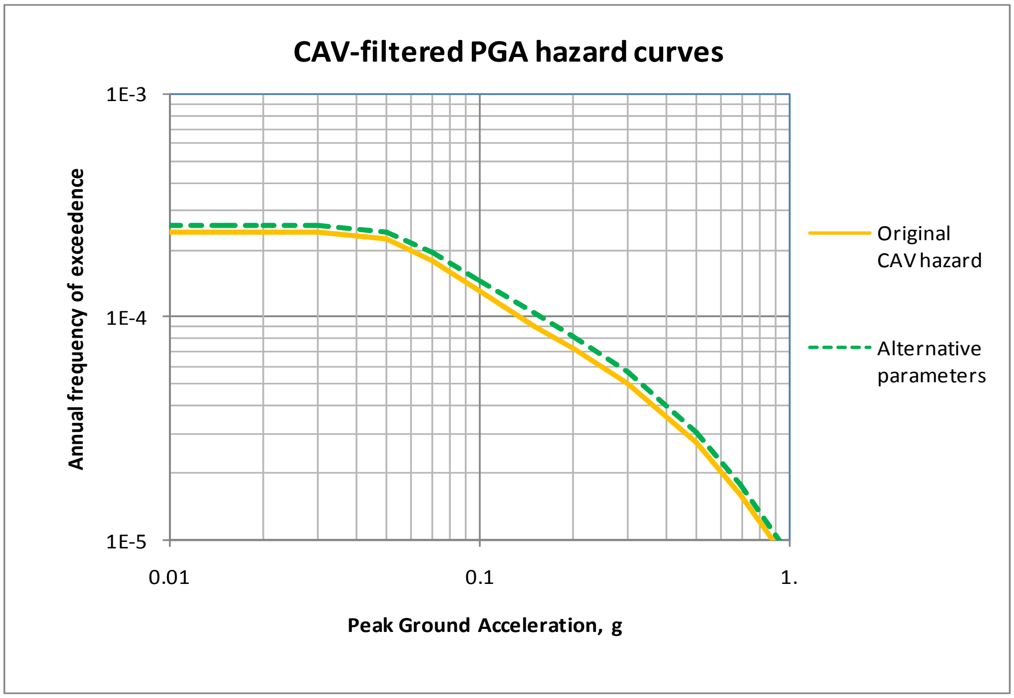


**Figure 15A: PGA hazard curves using CAV filter for original analysis and for alternative parameters.**

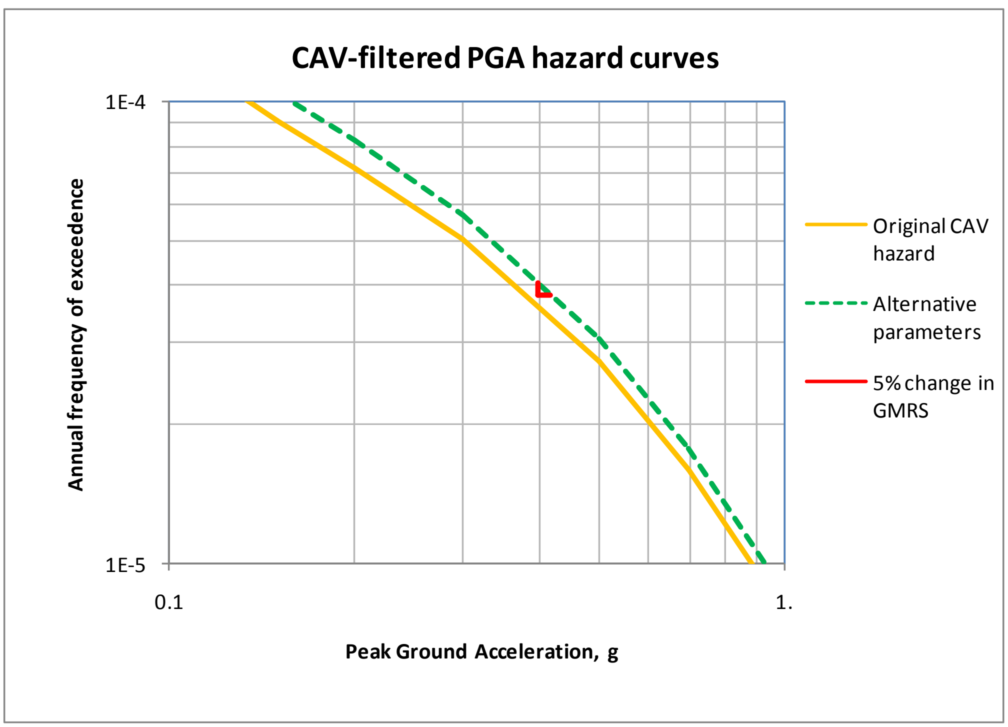


**Figure 15B: PGA hazard curves from Figure 15A expanded to show only one order of magnitude on amplitude and frequency axes. The red triangle shows the change in amplitude and annual frequency when using the GMRS calculated from the original analysis compared to the alternative parameters.**

## INTEGRATION OF ALTERNATIVE INTERPRETATIONS

As mentioned above, it would not be appropriate to discard the $m_{max}$ distributions for the ETSZ sources from the EPRI-SOG study entirely and substitute the alternative $m_{max}$ distribution. The alternative $m_{max}$ distribution was not developed as a result of earthquake occurrences in the region or a widely adopted theory, but rather represents alternative interpretations of two studies.

One reasonable way to include the alternative $m_{max}$ distribution would be to say that it represents 2 additional studies (representing 2 additional teams) that should be added to the composite hazard calculation. This can be achieved by calculating the hazard for the 6 EPRI-SOG teams, giving this hazard 75% weight (6 teams out of 8), and calculating the hazard the for EPRI-SOG teams with the alternative $m_{max}$ distribution and giving this hazard 25% weight (representing 2 additional teams out of 8). Both calculations would use the updated seismicity parameters through 2006 to represent the extended earthquake catalog. This is designated here the "integrated calculation."

Table 5 compares the $10^{-4}$ and $10^{-5}$ UHRS amplitudes and the GMRS amplitudes for the original EPRI-SOG assumptions and for the integrated calculation using the non-CAV hazard. Table 6 shows a similar comparison between the original CAV-filtered hazard and the integrated, CAV-filtered hazard.

**Table 5: Comparison between GMRS and UHRS at test site for EPRI-SOG parameters and integrated $m_{max}$ values, non-CAV hazard (note: % differences were calculated with more decimal places than are shown in the tables).**

| Freq. (Hz) | Orig 1E-4 (g) | Orig 1E-5 (g) | GMRS (g) | Alt. 1E-4 (g) | Alt. 1E-5 (g) | GMRS (g) | % DIFF |
|---|---|---|---|---|---|---|---|
| 100 | 0.264 | 0.875 | 0.413 | 0.266 | 0.881 | 0.416 | 0.7% |
| 25 | 0.725 | 2.45 | 1.15 | 0.730 | 2.46 | 1.16 | 0.7% |
| 10 | 0.480 | 1.48 | 0.709 | 0.483 | 1.49 | 0.713 | 0.6% |
| 5 | 0.306 | 0.896 | 0.434 | 0.307 | 0.899 | 0.435 | 0.4% |
| 2.5 | 0.173 | 0.454 | 0.225 | 0.174 | 0.453 | 0.225 | 0.0% |
| 1 | 0.0894 | 0.217 | 0.109 | 0.0894 | 0.216 | 0.109 | -0.4% |
| 0.5 | 0.0615 | 0.165 | 0.0814 | 0.0614 | 0.165 | 0.0811 | -0.4% |

**Table 6: Comparison between GMRS at test site for EPRI-SOG parameters and integrated $m_{max}$ values, CAV-filtered hazard (note: % differences were calculated with more decimal places than are shown in the tables).**

| Freq. (Hz) | Orig 1E-4 (g) | Orig 1E-5 (g) | GMRS (g) | Alt. 1E-4 (g) | Alt. 1E-5 (g) | GMRS (g) | % DIFF |
|---|---|---|---|---|---|---|---|
| 100 | 0.135 | 0.885 | 0.398 | 0.136 | 0.893 | 0.402 | 0.9% |
| 25 | 0.351 | 2.43 | 1.09 | 0.355 | 2.45 | 1.10 | 1.0% |
| 10 | 0.257 | 1.43 | 0.644 | 0.259 | 1.44 | 0.648 | 0.7% |
| 5 | 0.191 | 0.842 | 0.379 | 0.192 | 0.845 | 0.380 | 0.4% |
| 2.5 | 0.114 | 0.422 | 0.195 | 0.114 | 0.421 | 0.195 | -0.1% |
| 1 | 0.0545 | 0.202 | 0.0933 | 0.0544 | 0.201 | 0.0929 | -0.5% |
| 0.5 | 0.0302 | 0.149 | 0.0672 | 0.0301 | 0.148 | 0.0668 | -0.6% |

Tables 5 and 6 show that when the alternative $m_{max}$ distribution is integrated into a total seismic hazard analysis with a weighting that represents the additional studies, the effect ranges from a 0.6% decrease to a 1.0% increase in GMRS. The decrease in GMRS results from extending the seismicity catalog from 1985 to 2006, during which time the mean rate of earthquake activity has decreased in the ETSZ. The effect of $m_{max}$ is smallest for long period measures of ground motion, for which the New Madrid faults have an important contribution to hazard (see the plots in Appendix A). Figure 16 plots the PGA hazard curves for the original and integrated analyses using the CAV filter. The curves are so close that they cannot be distinguished when plotted on the common scale of two orders of magnitude for annual frequency and for ground motion amplitude.

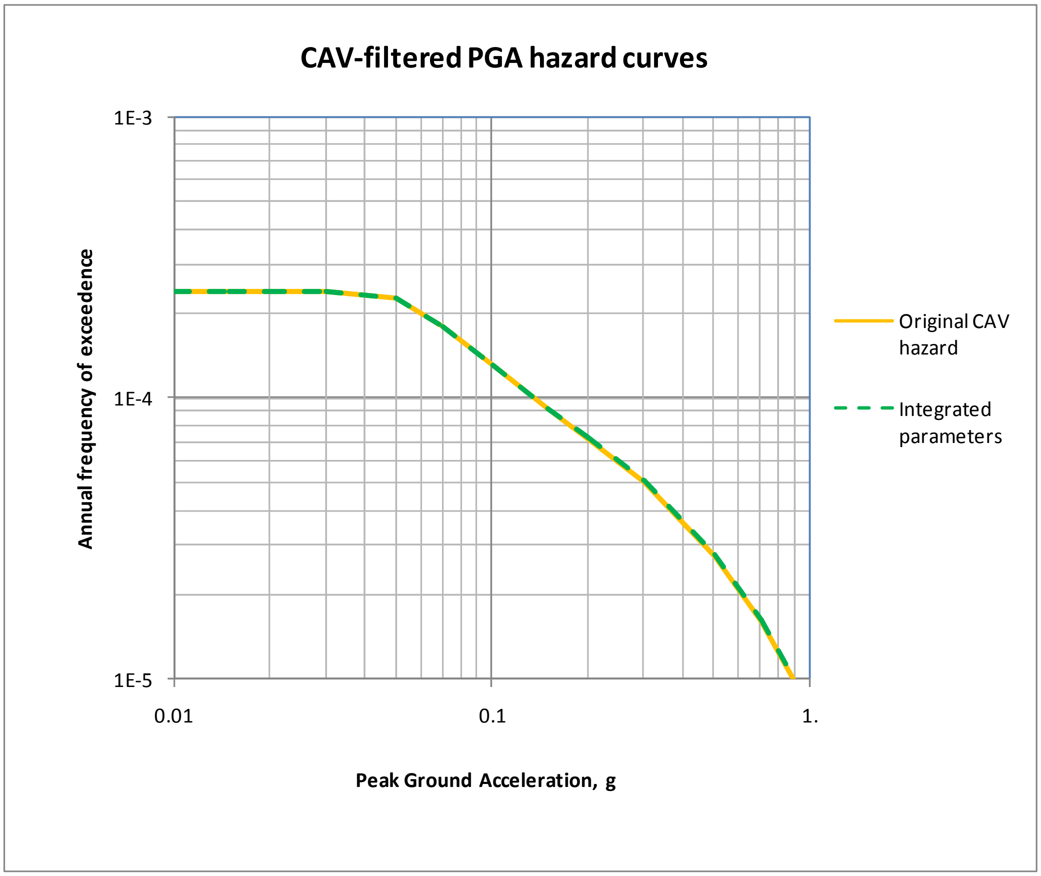


**Figure 16: PGA hazard curves using CAV filter for original analysis and for integrated parameters.**

It should be noted that GMRS amplitudes calculated for plant license applications are generally reported to 3 significant figures, which corresponds to a precision of ±1% (for example, a GMRS amplitude of 1.00499 would be reported as 1.00, and an amplitude of 1.005 would be reported as 1.01, a precision of 1%). Thus the effect of the integrated calculation summarized in Tables 5 and 6 results in changes to GMRS amplitudes that are on the same order as the precision with which GMRS calculations are generally reported.

## CONCLUSIONS

Differences in maximum magnitude distributions for the ETSZ between the EPRI-SOG study and more recent studies (the TIP and DSS studies) indicate that alternative interpretations of $m_{max}$ have a higher mean value than was assessed in the EPRI-SOG study. Adopting this alternative distribution for ETSZ sources would increase seismic hazard estimates for a site located within the ETSZ. A compensating effect would be that more recent seismicity since the EPRI-SOG study indicates lower mean rates of activity in the ETSZ. Overall, combining the alternative $m_{max}$ distributions into an integrated analysis that accounts for changes in mean rates of earthquake activity leads to estimates of changes in GMRS amplitude for a site within the ETSZ between -0.6% and +1.0%. These changes are on the same order of precision with which

GMRS amplitudes are generally reported in nuclear plant license applications. The conclusion is that the potential change in GMRS resulting from integrating the alternative $m_{max}$ distribution into the analysis is not significant, compared to GMRS amplitudes calculated using the EPRI-SOG (1989) $m_{max}$ distributions and activity rates.

These conclusions support the basis for no adjustments to the ETSZ as currently documented in the ESP and COL applications submitted to date.

## REFERENCES


1. LLNL (2002). *Guidance for Performing Probabilistic Seismic Hazard Analysis for a Nuclear Plant Site: Example Application to the Southeastern United States*, USNRC Rept. NUREG/CR-6607, Oct.
2. Geomatrix Consultants (2004). *Dam Safety Seismic Hazard Assessment*, report prepared for Tennessee Valley Authority, 2 vol, September.
3. Tennessee Valley Authority (2007). *Bellefonte Units 3 & 4 COLA (Final Safety Analysis Report) Rev. 0 Chapter 02, Site Characteristics*, US Nuc. Reg. Comm. document accession no. ML073110902, Oct. 30.
4. Gardner, J.K., and L. Knopoff (1974). Is the sequence of earthquakes in southern California, with aftershocks removed, Poissonian? *Bull. Seism. Soc. Am., 64, 1363-1367.*
5. Risk Engineering, Inc. (1989). *EQHAZARD Primer*, EPRI Rept. NP-6452-D, Special Report, June.
6. Atkinson, G.M., and D.M. Boore (1995). "Ground motion relations for eastern North America", *Bull. Seism. Soc. Am,* 85, 1, 17-30.
7. Frankel, A., C. Mueller, T. Barnhard, D. Perkins, E.V. Leyendecker, N. Dickman, S. Hanson, and M. Hooper (1996). *National seismic hazard maps: documentation*, US Geol. Survey Open-file Rept. 96-532.
8. EPRI (1993). *Guidelines for determining design basis ground motions, Vol. 5: Quantification of seismic source effects*, EPRI Rept. TR-102293, Nov.
9. Exelon (2003). *09/25/03-Submittal of Exelon Generation Company (EGC) application for an early site permit (ESP) for property co-located with existing Clinton Power Station (CPS) facility in Illinois,* US Nuc. Reg. Comm. document accession no. ML032721596, Sept. 25.
10. Southern Nuclear Co (2008). *Vogtle Early Site Permit Application, Revision 4, Part 2 – Site Safety Analysis Report, Chapter 2, "Site Characteristics," Section 2.5.2,* US Nuc. Reg. Comm. document accession no. ML081020220, March 28.
11. EPRI (2004). *CEUS ground motion project final report*, Elec. Power Res. Inst, Palo Alto, Rept. 1008910, Dec.
12. Abrahamson, N.A., and J. Bommer (2006). *Program on technology innovation: truncation of the lognormal distribution and value of the standard deviation for ground motion models in the Central and Eastern United States*, Elec. Power Res. Inst, Palo Alto, Rept. 1014381, Aug.
13. Hardy, G, K. Merz, N. Abrahamson, and J. Watson-Lamprey (2006). *Program on Technology Innovation: Use of Cumulative Absolute Velocity (CAV) in Determining Effects of Small Magnitude Earthquakes on Seismic Hazard,* Elec. Power Res. Inst, Palo Alto, Rept. 1014099.
14. EPRI (1989). *Probabilistic Seismic Hazard Evaluations at Nuclear Plant Sites in the Central and Eastern United State: Resolution of the Charleston Earthquake Issue*, Elec. Power Res. Inst., Palo Alto, EPRI Rept. NP-6395-D, April.

# APPENDIX A

## Hazard curves by source for each EPRI-SOG Team for non-CAV calculation, updated rates and alternative $M_{max}$.

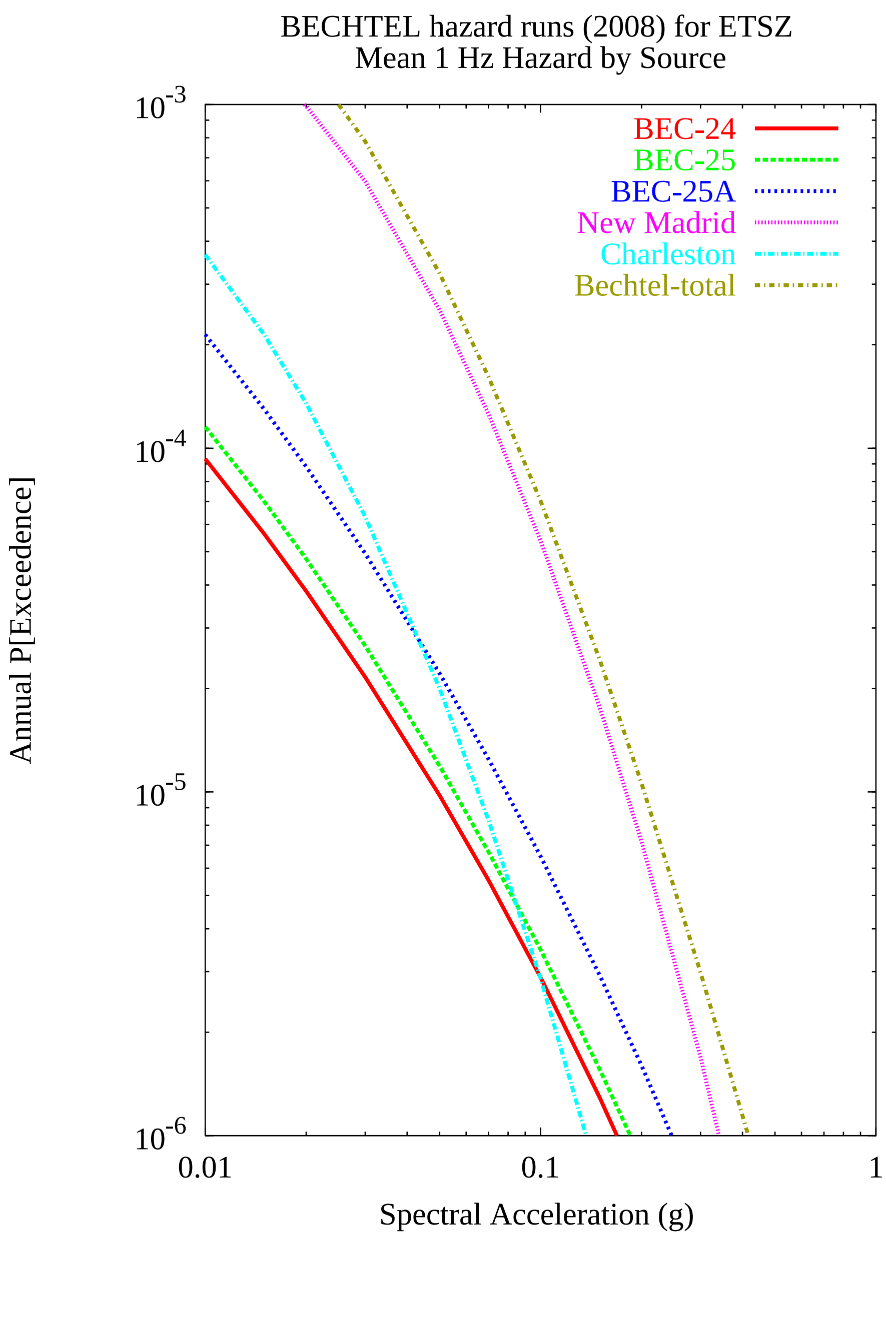


**Figure A1: Bechtel 1 Hz hazard**

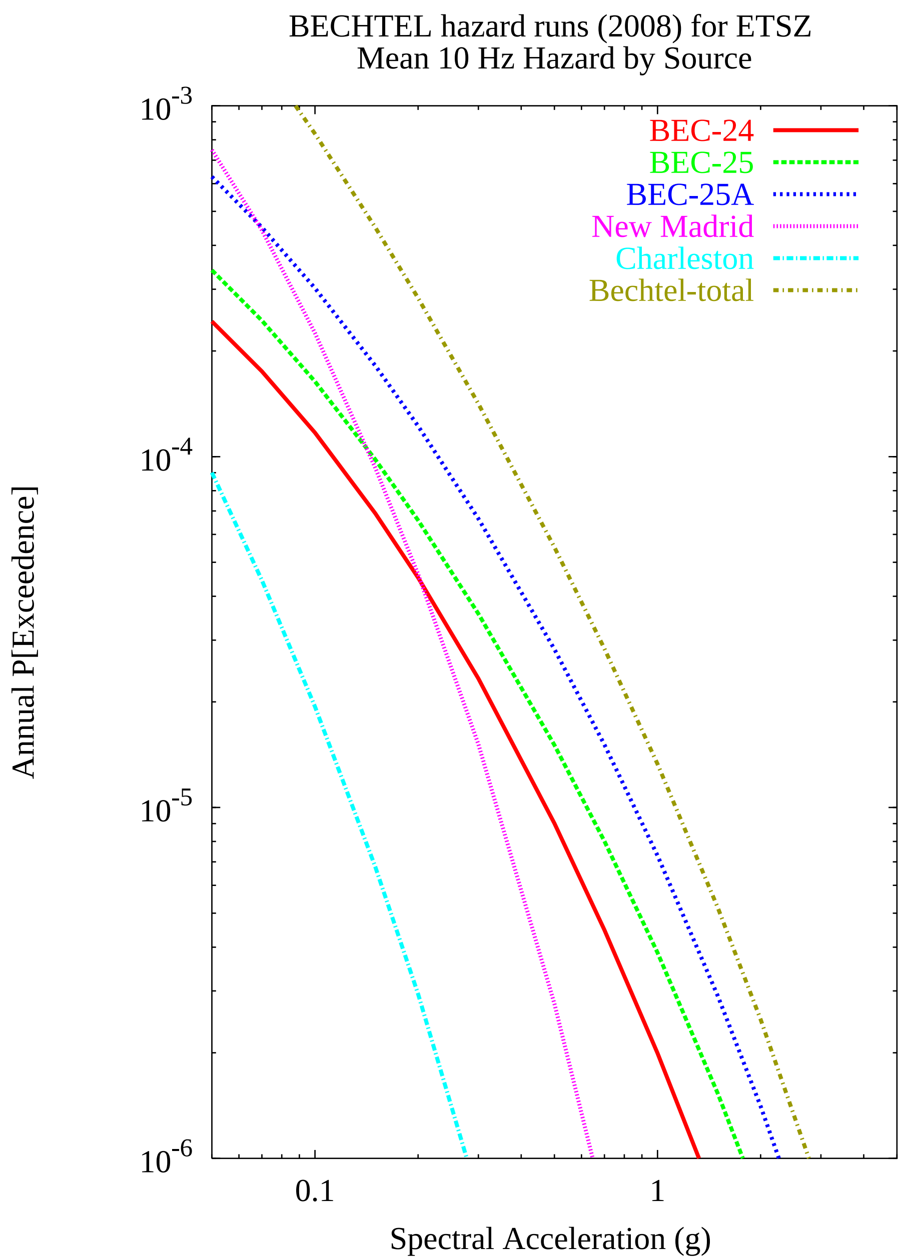


**Figure A2: Bechtel 10 Hz hazard**

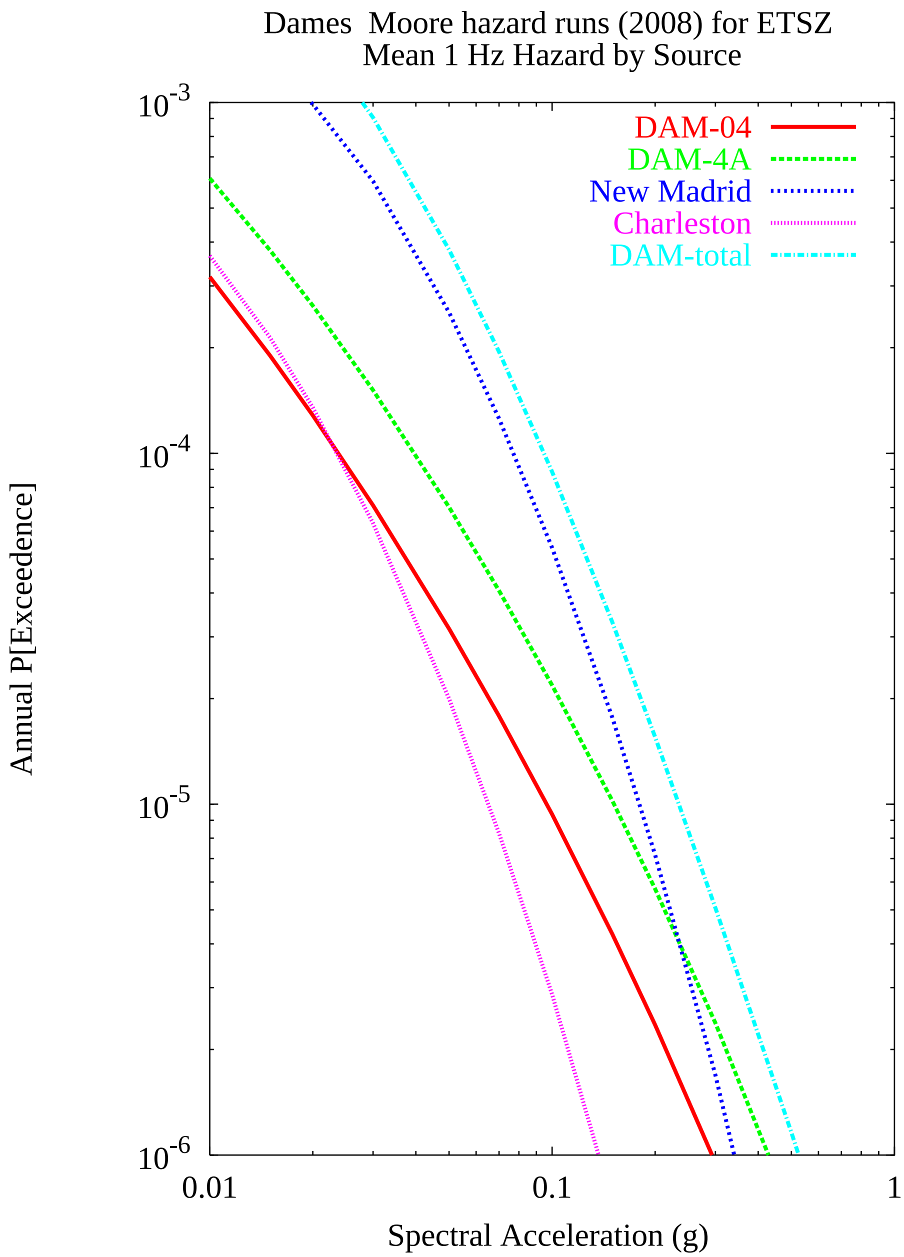


**Figure A3: Dames & Moore 1 Hz hazard**

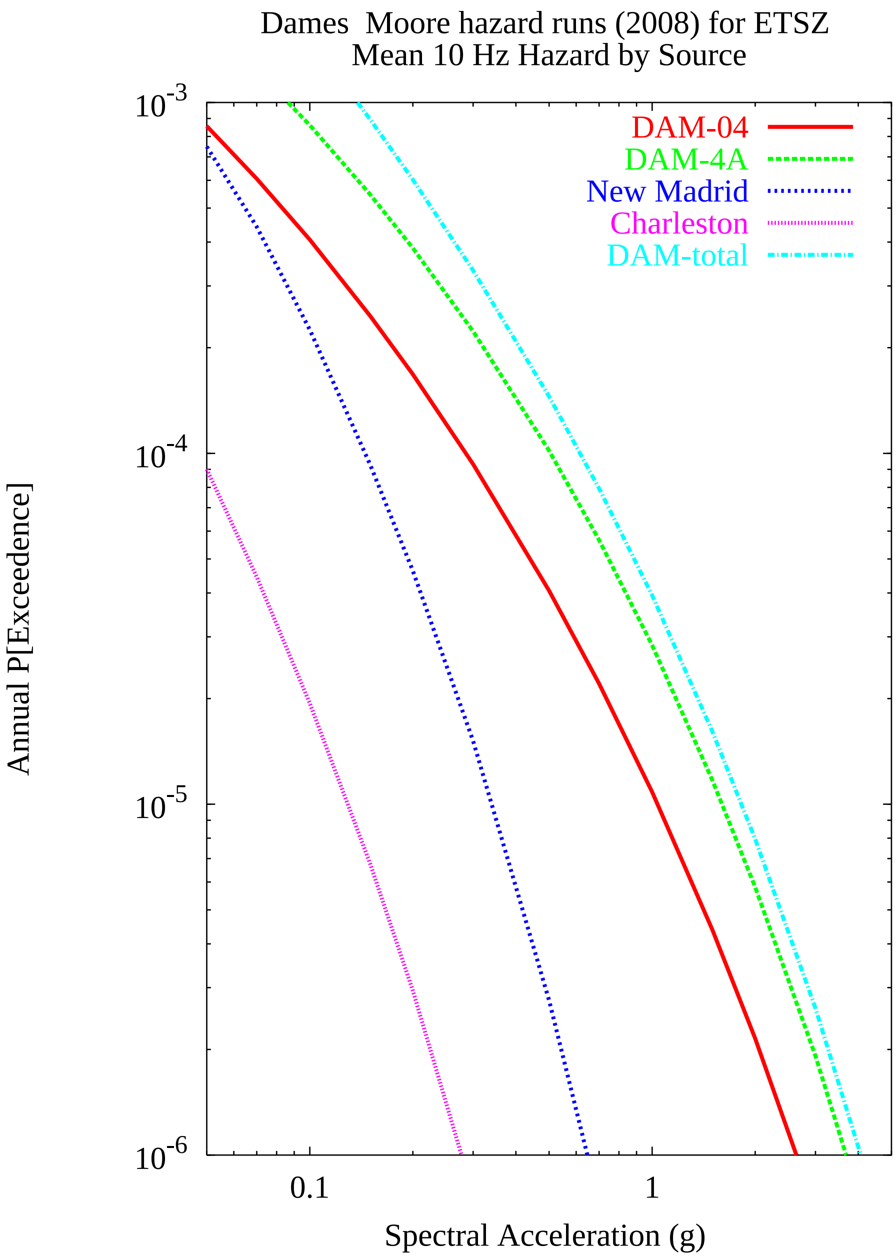


**Figure A4: Dames & Moore 10 Hz hazard**

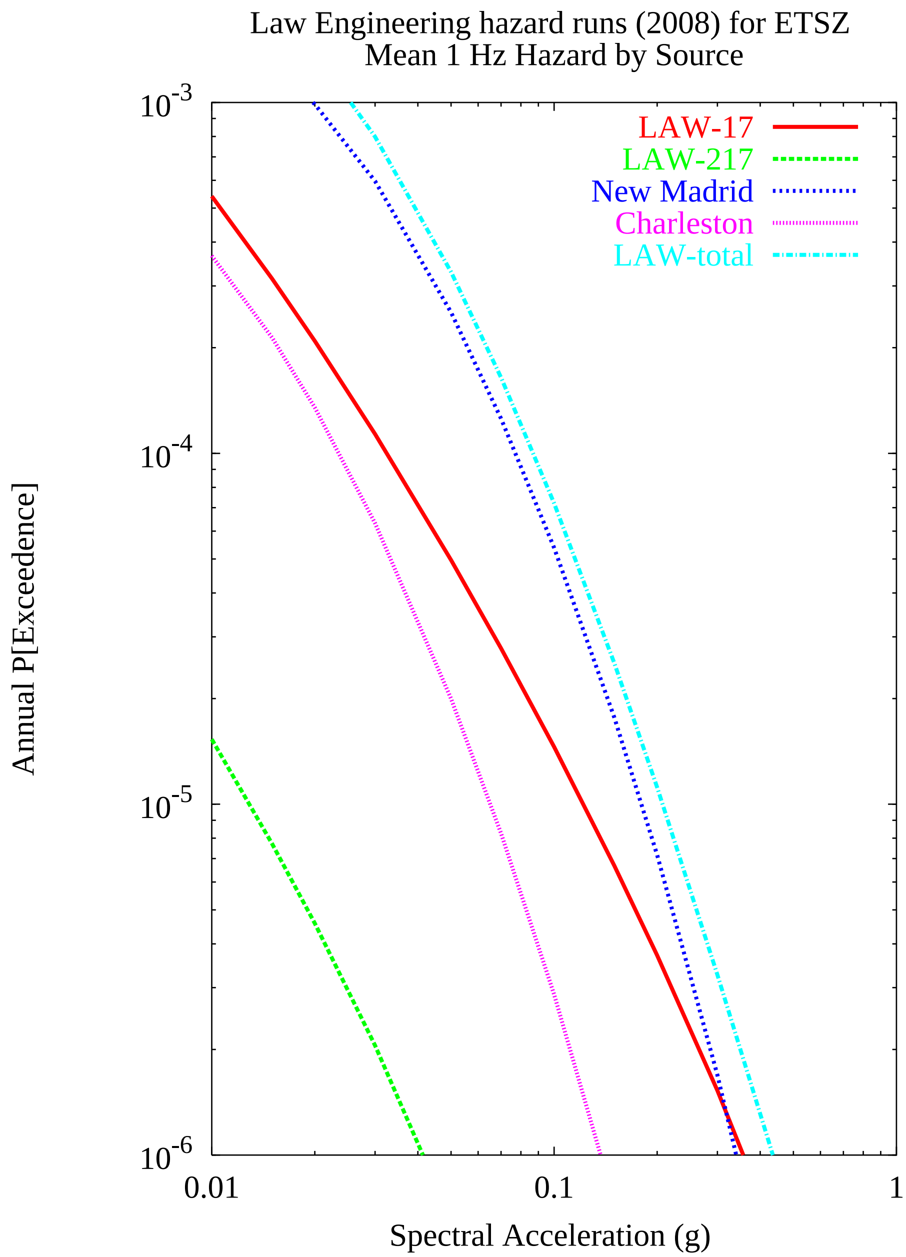


**Figure A5: Law 1 Hz hazard**

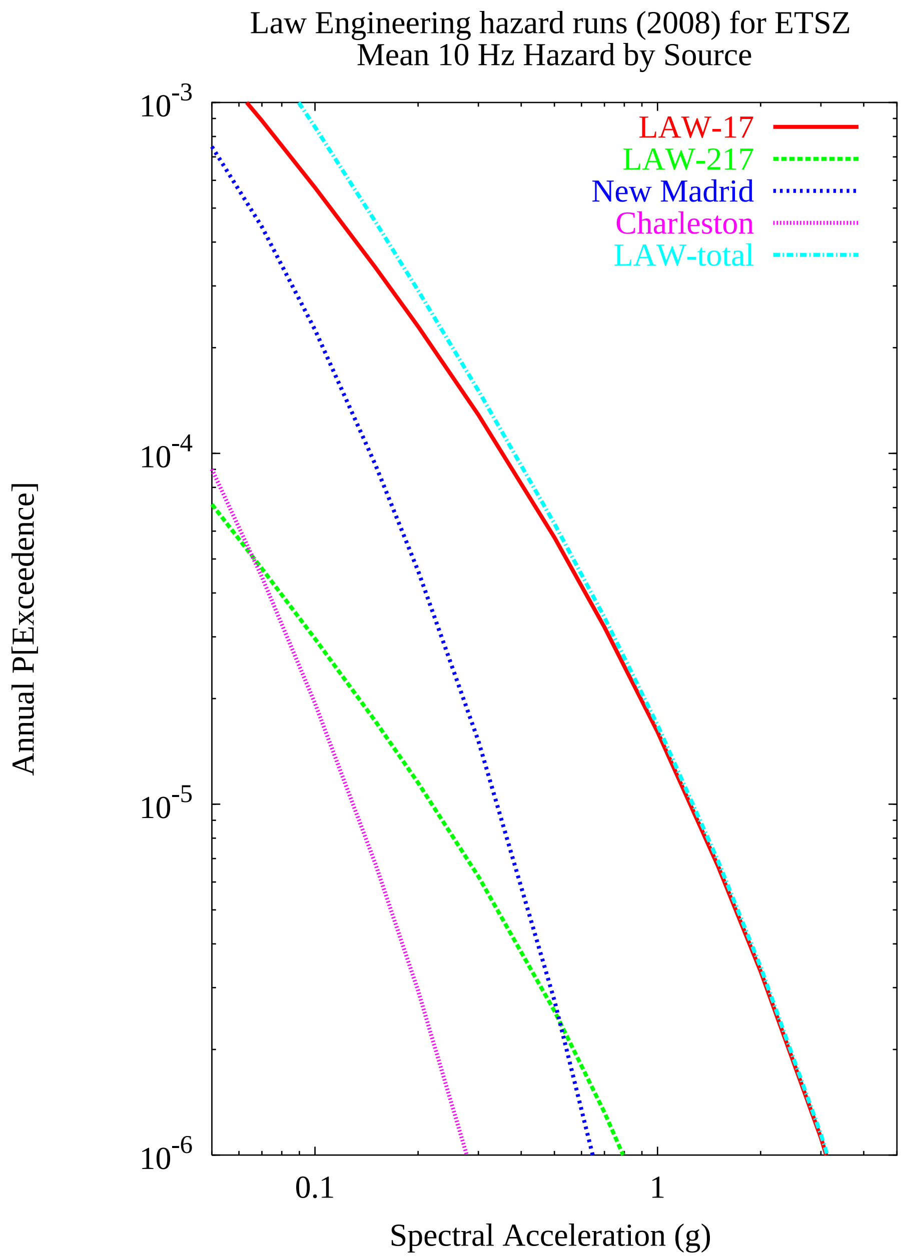


**Figure A6: Law 10 Hz hazard**

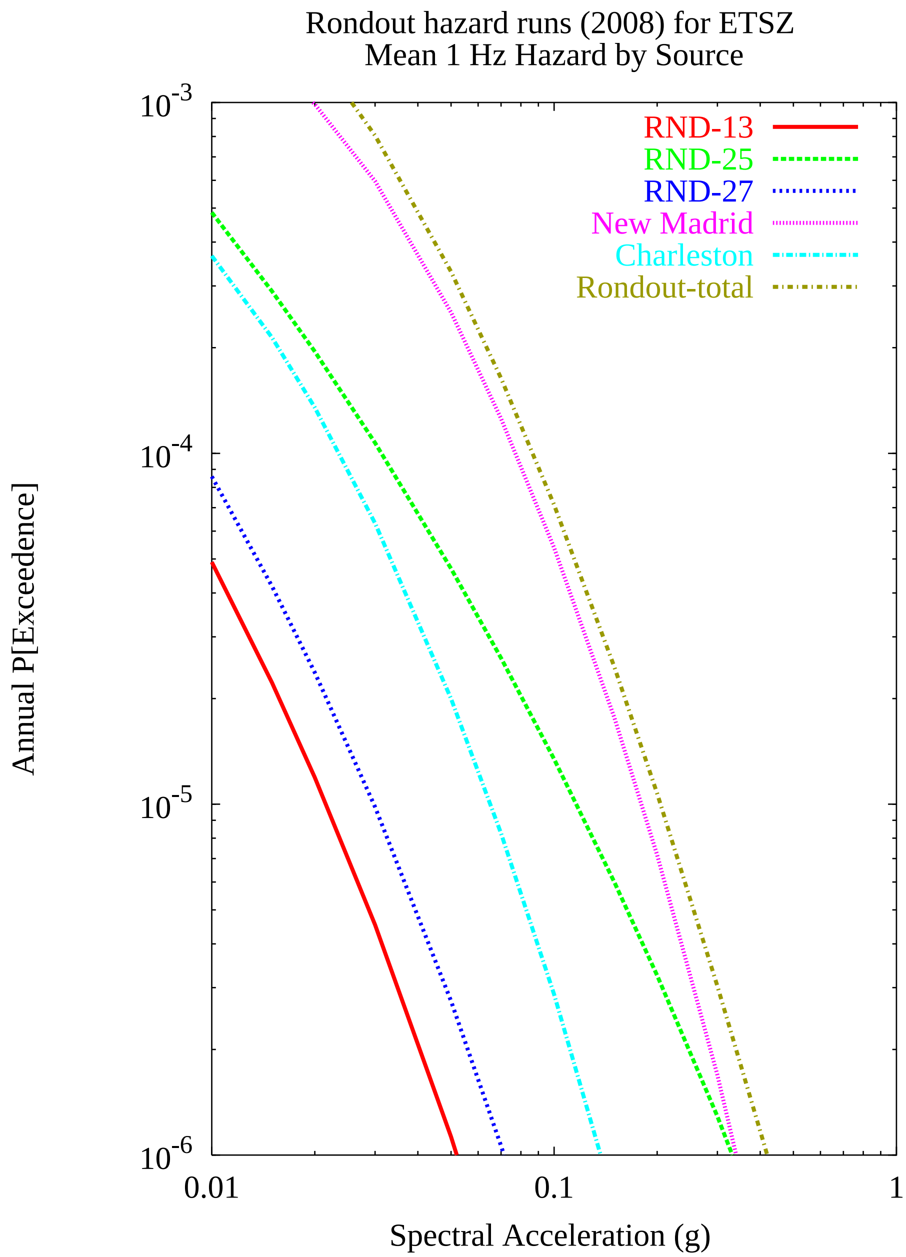


**Figure A7: Rondout 1 Hz hazard**

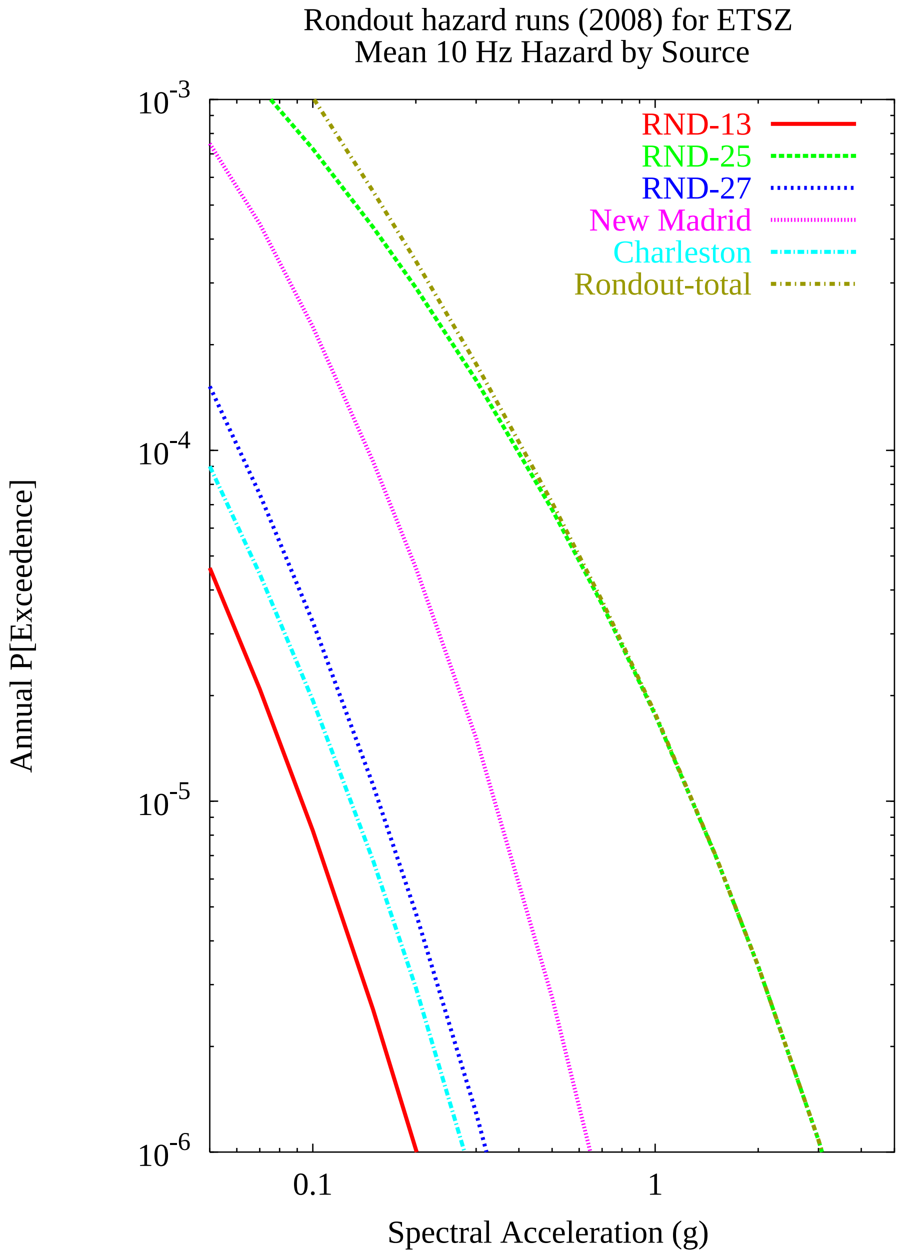


**Figure A8: Rondout 10 Hz hazard**

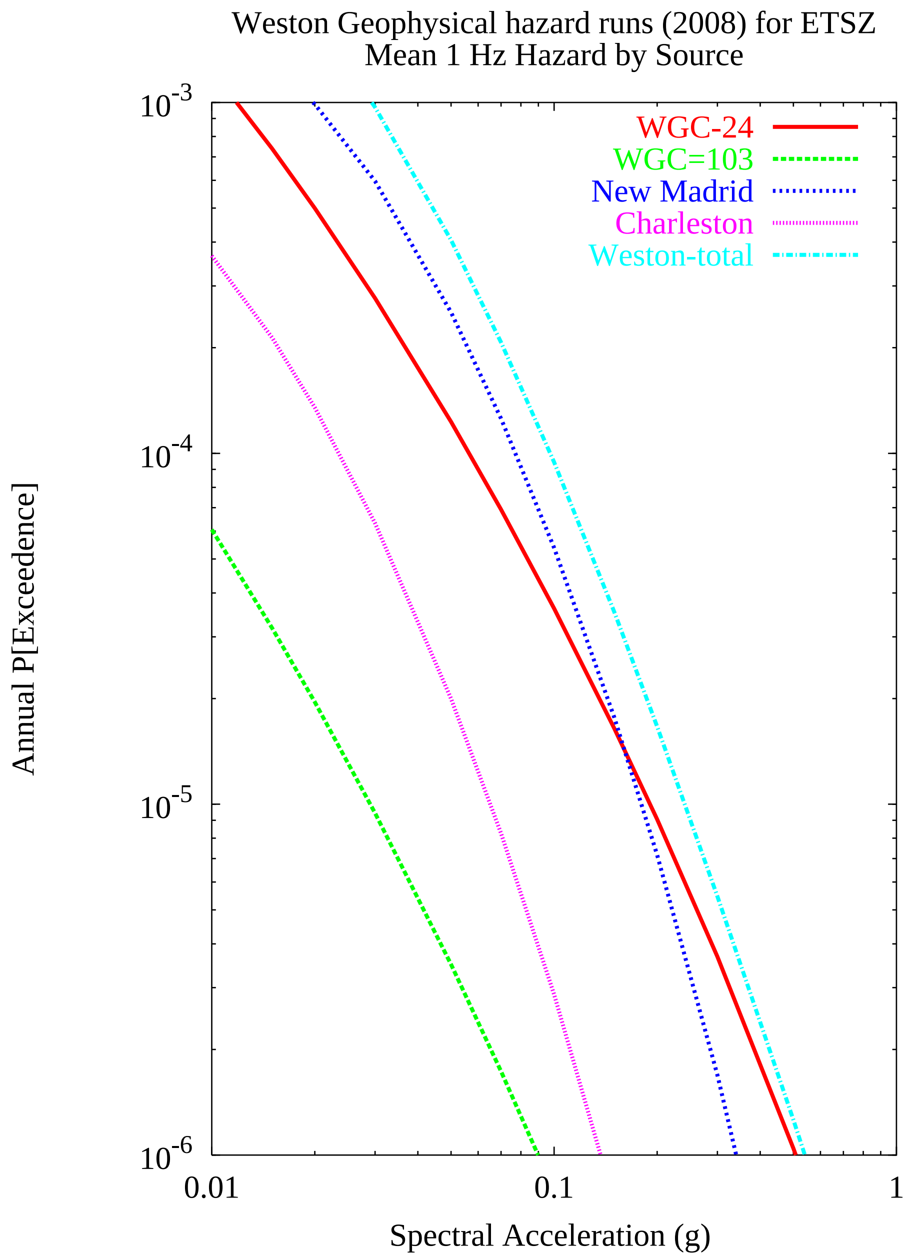


**Figure A9: Weston 1 Hz hazard**

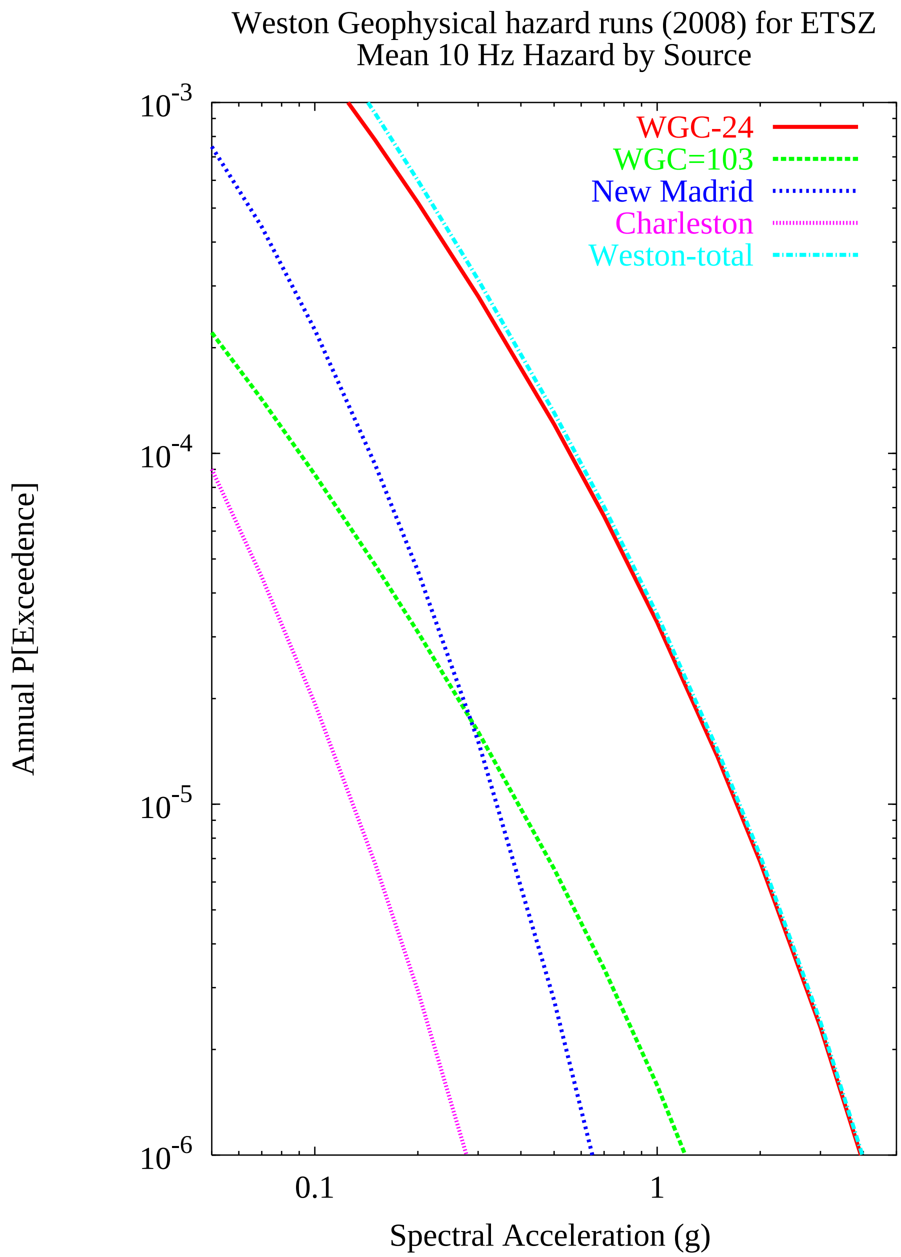


**Figure A10: Weston 10 Hz hazard**

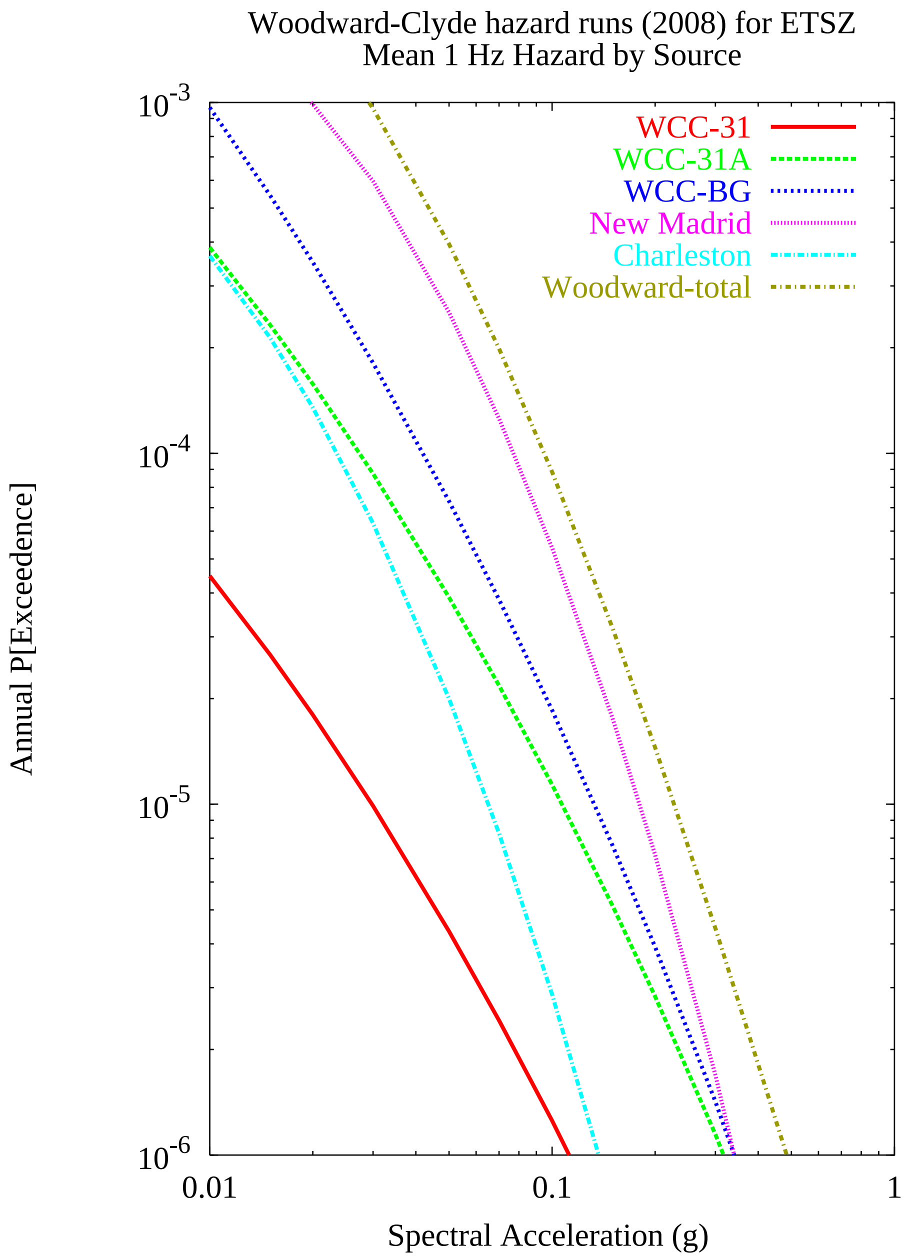


**Figure A11: Woodward-Clyde 1 Hz hazard**

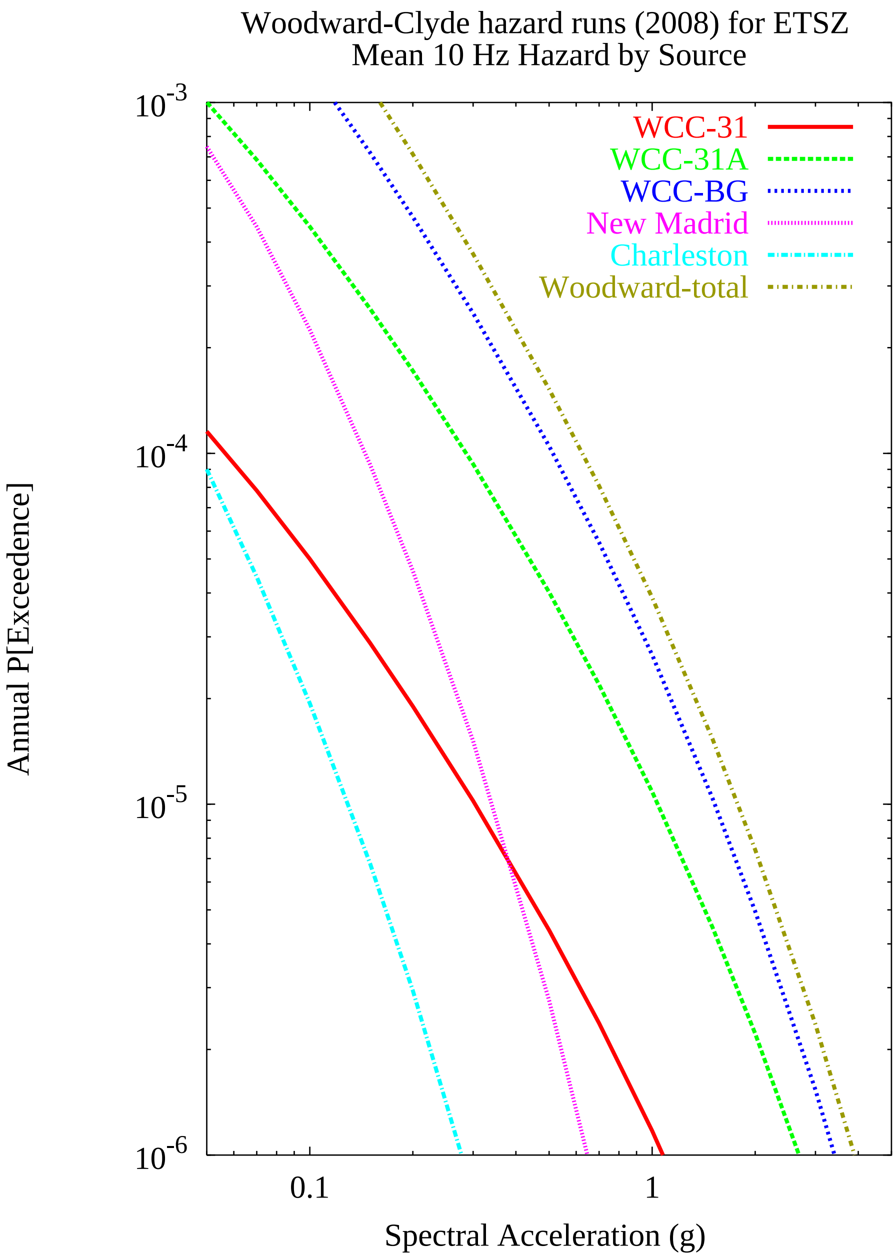


**Figure A12: Woodward-Clyde 10 Hz hazard**

# APPENDIX B

## Hazard curves by source for each EPRI-SOG Team for CAV calculation, updated rates and alternative $M_{max}$.

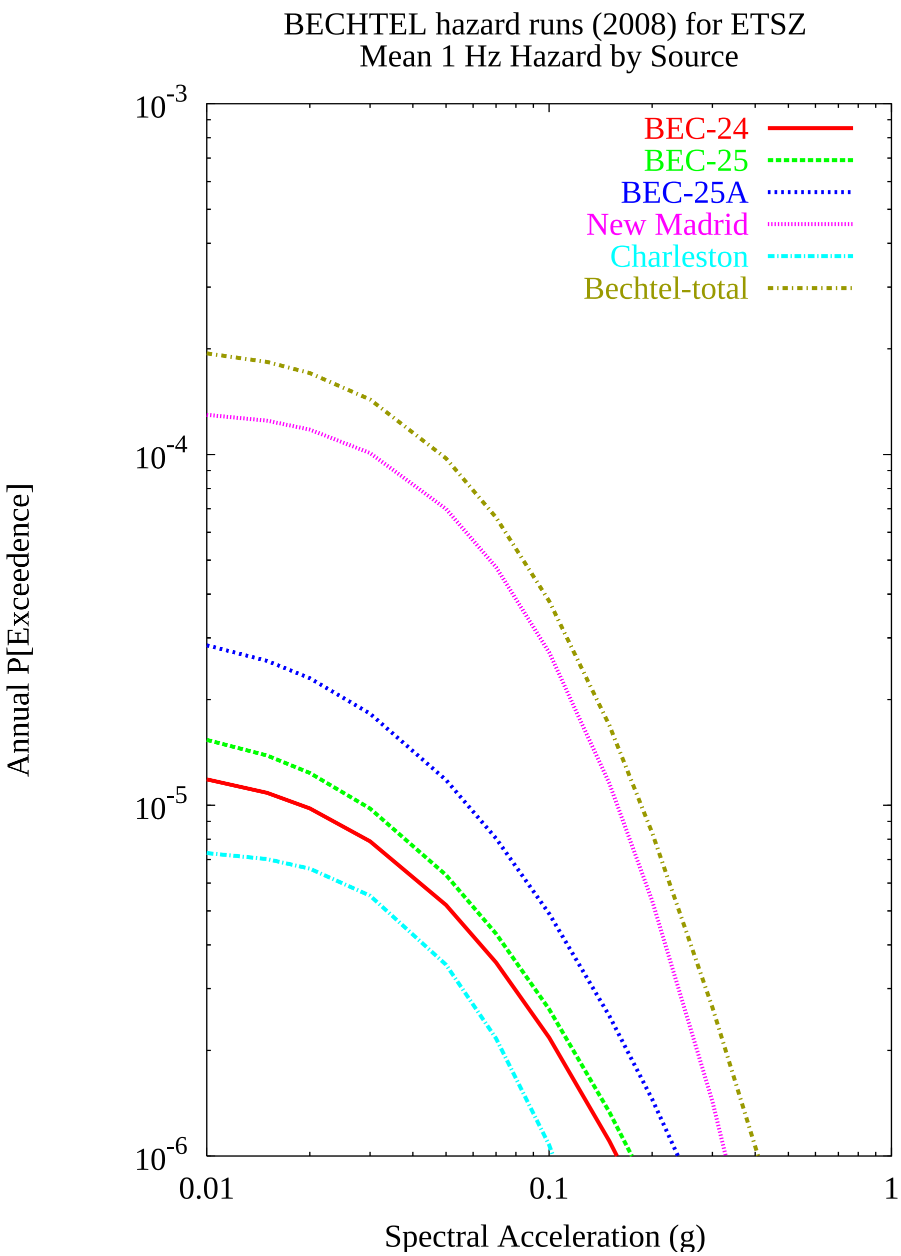


**Figure B1: Bechtel 1 Hz hazard**

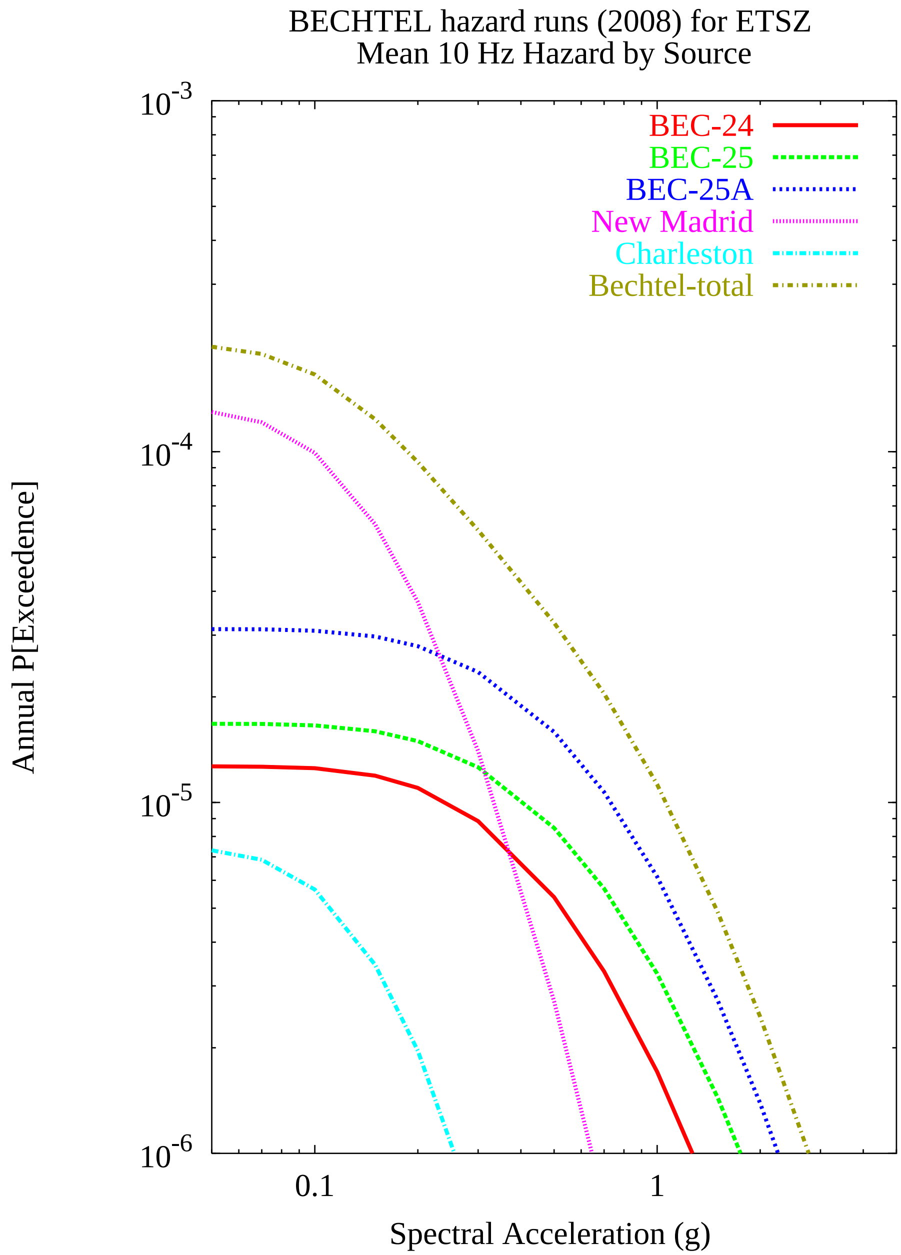


**Figure B2: Bechtel 10 Hz hazard**

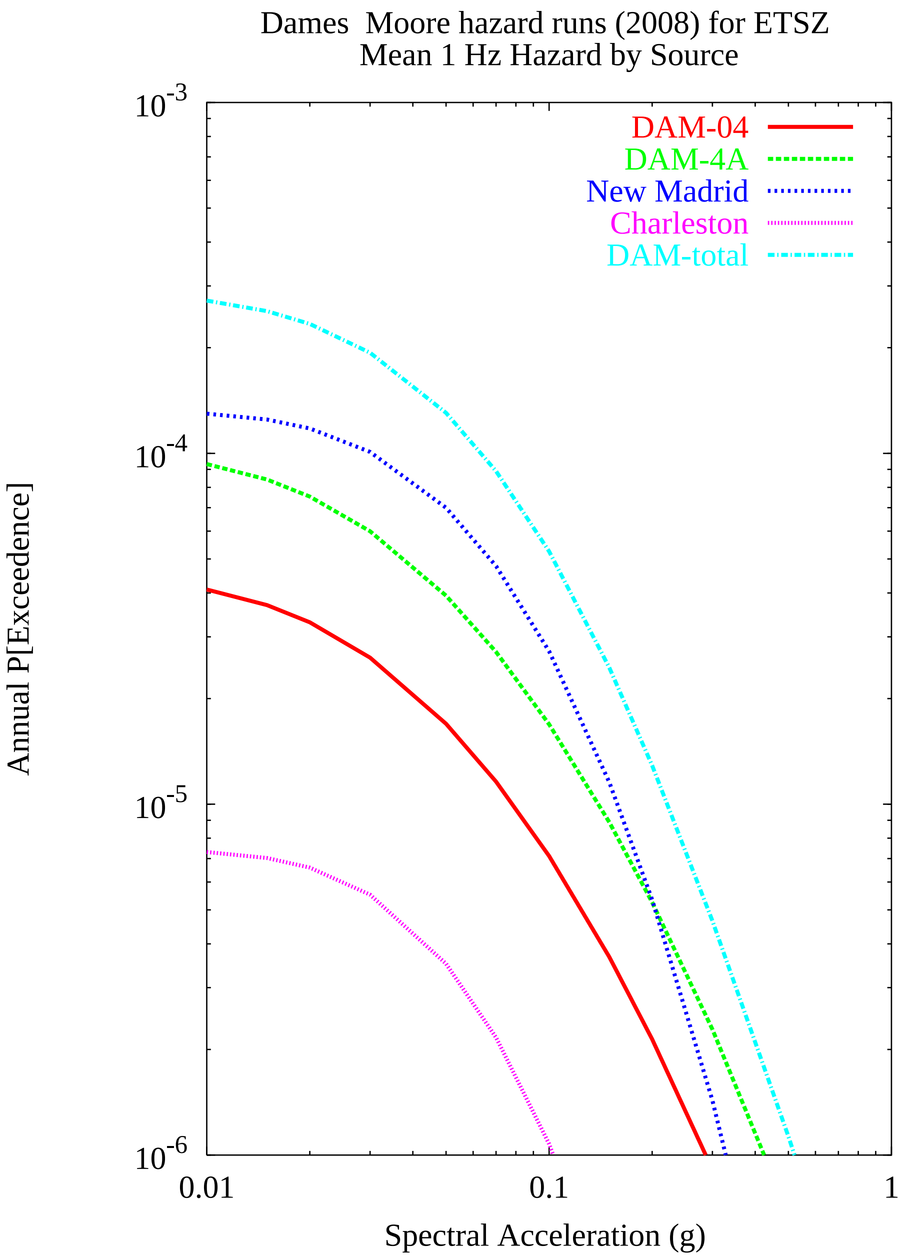


**Figure B3: Dames & Moore 1 Hz hazard**

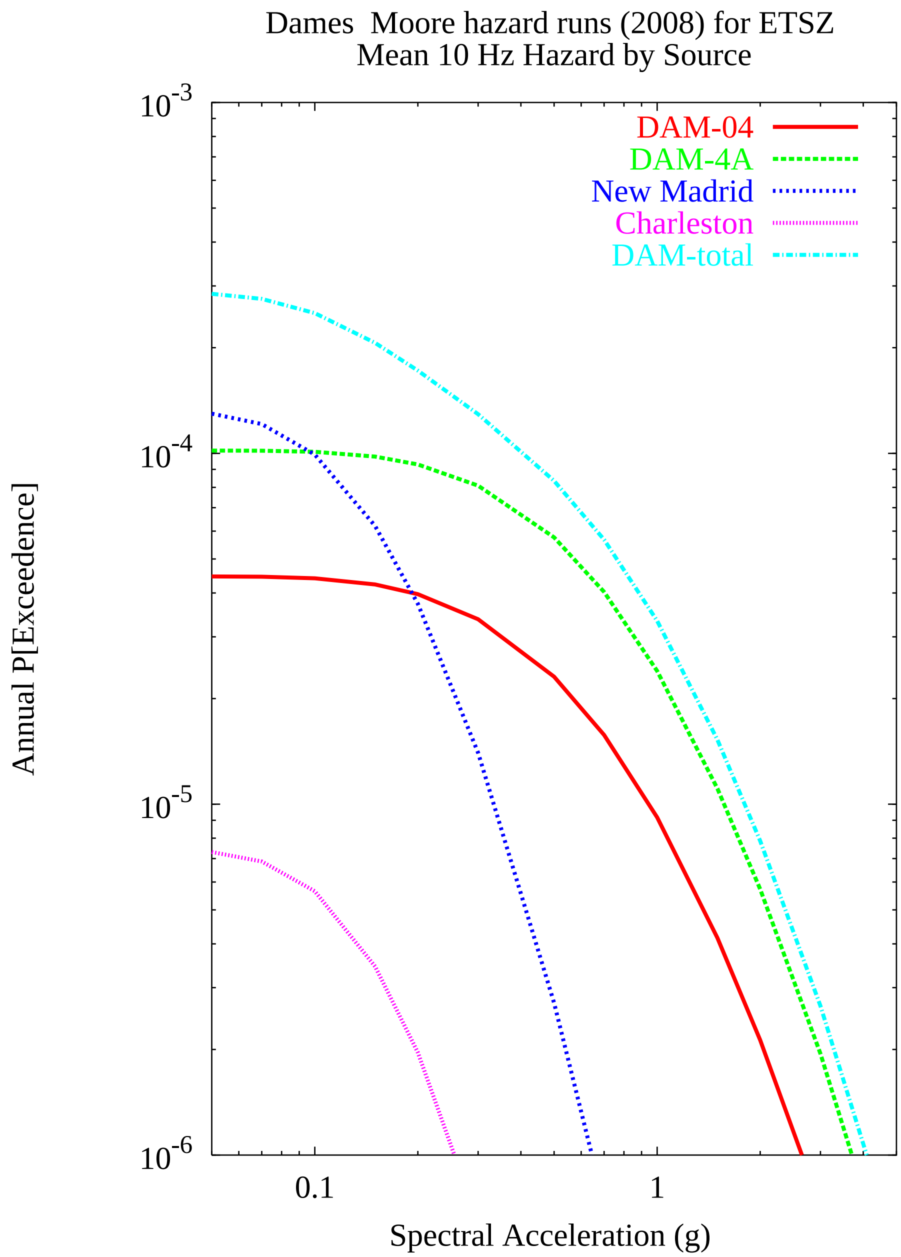


**Figure B4: Dames & Moore 10 Hz hazard**

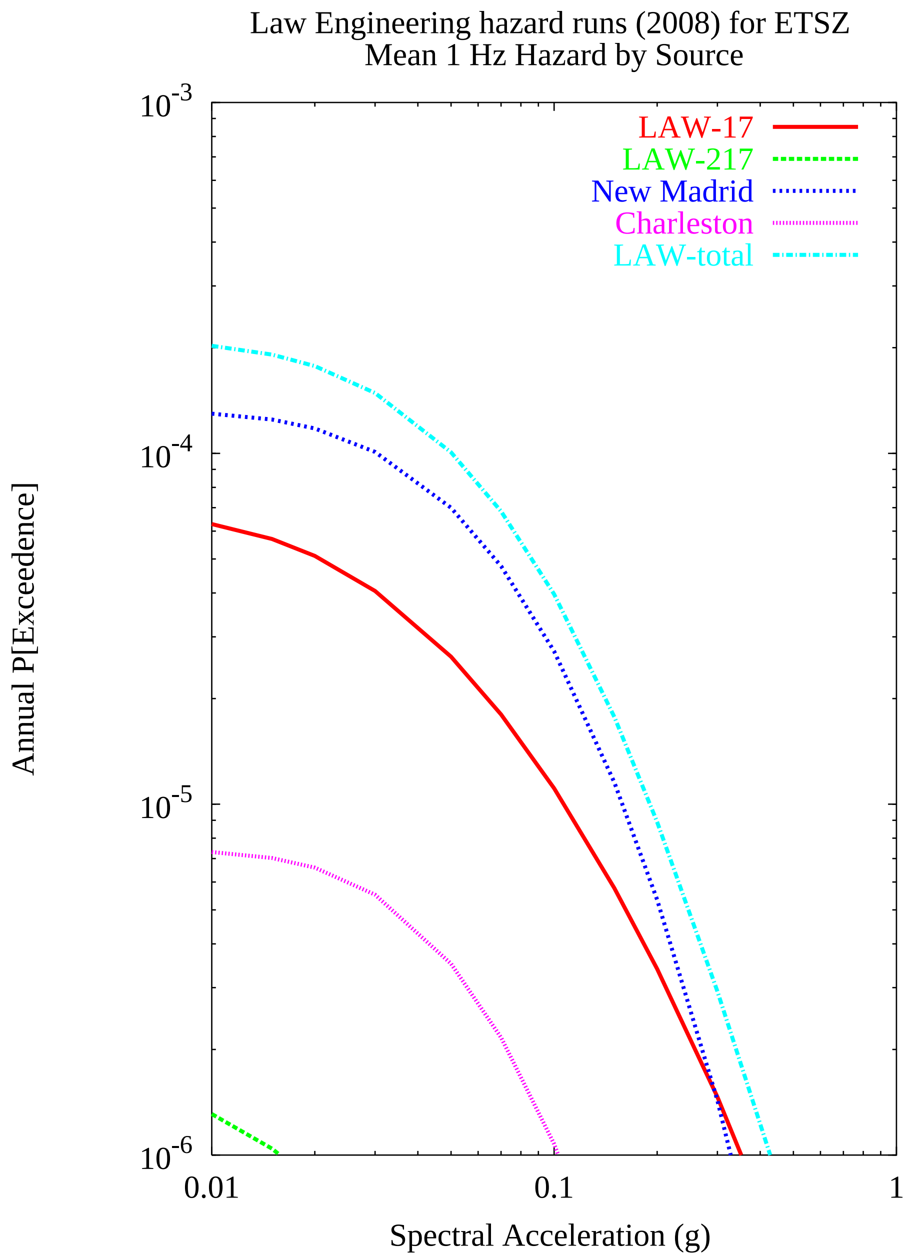


**Figure B5: Law 1 Hz hazard**

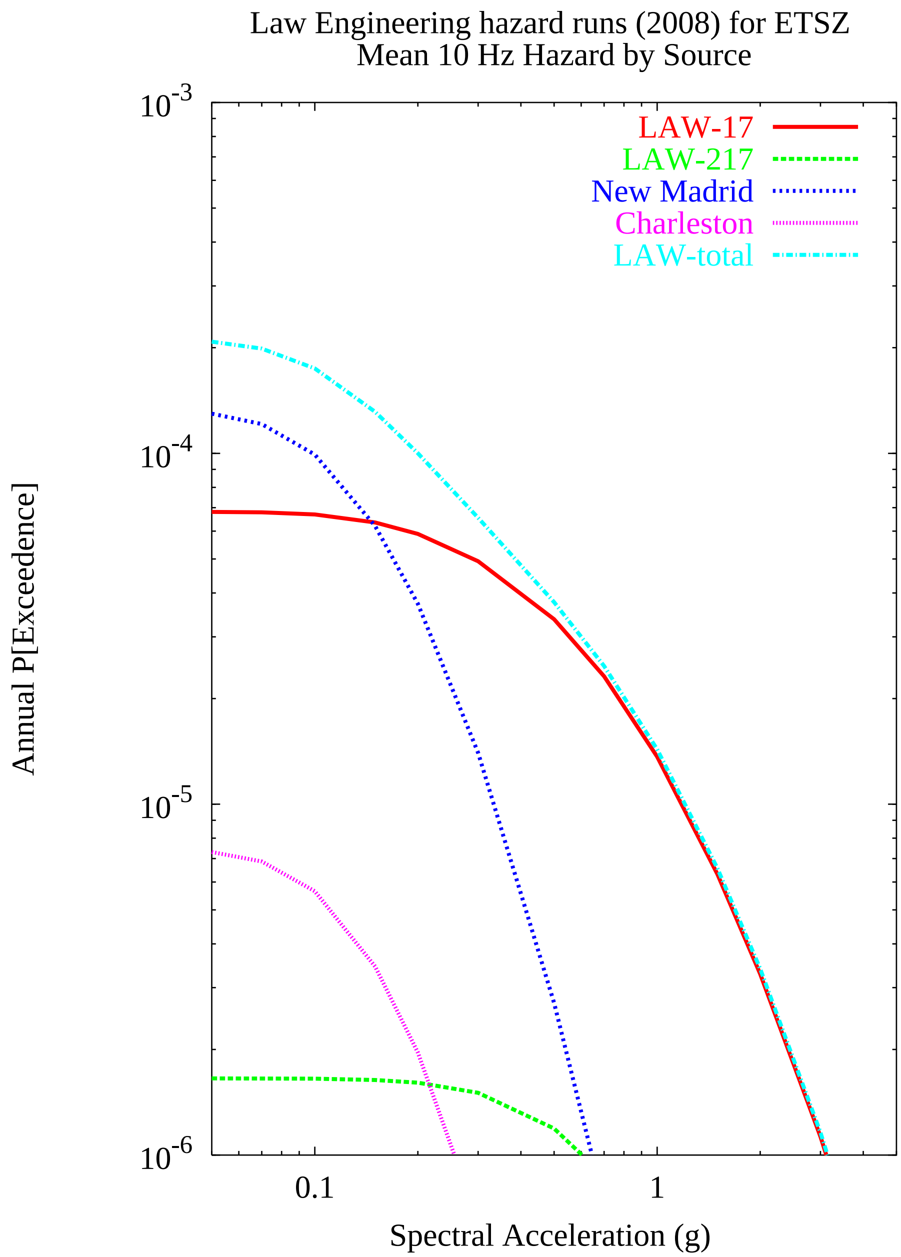


**Figure B6: Law 10 Hz hazard**

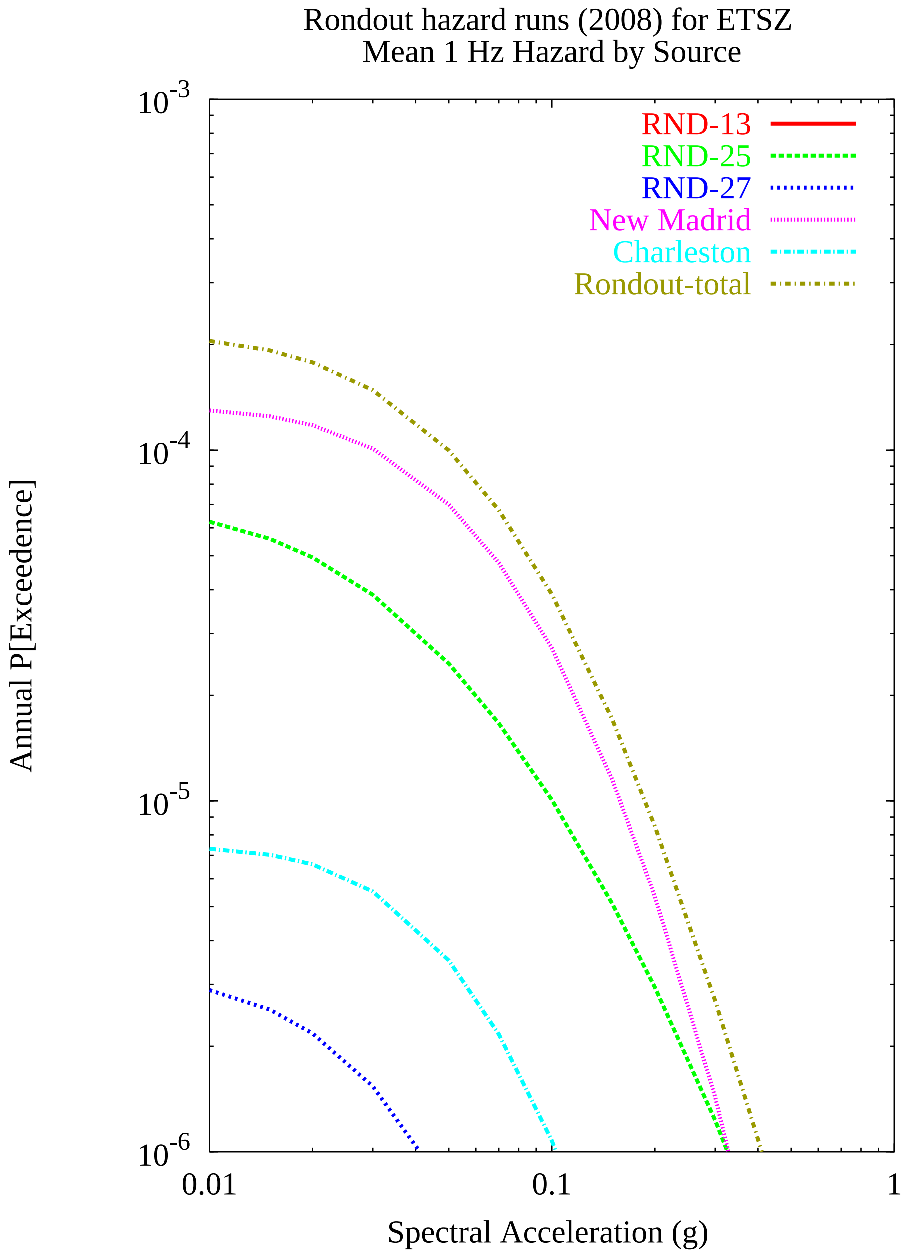


**Figure B7: Rondout 1 Hz hazard**

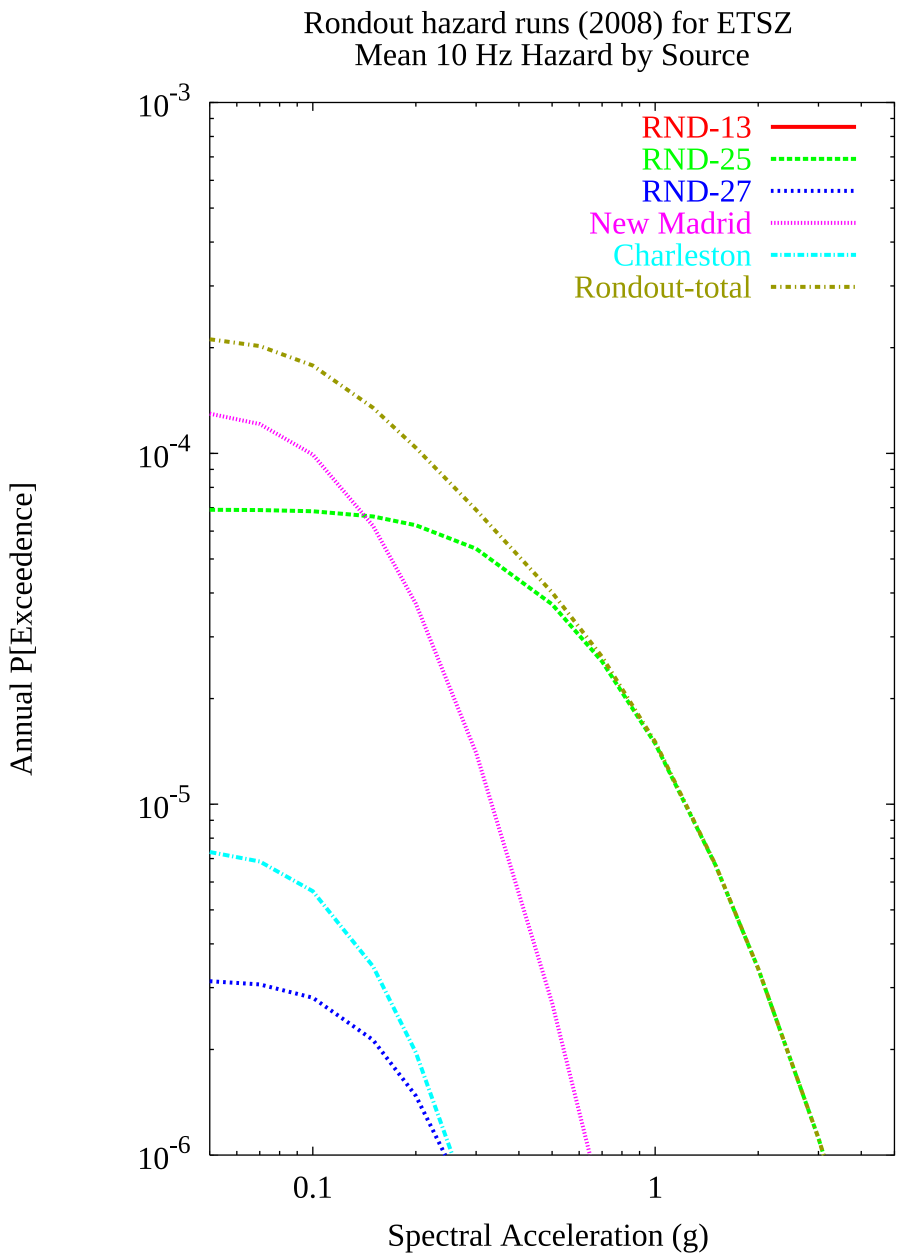


**Figure B8: Rondout 10 Hz hazard**

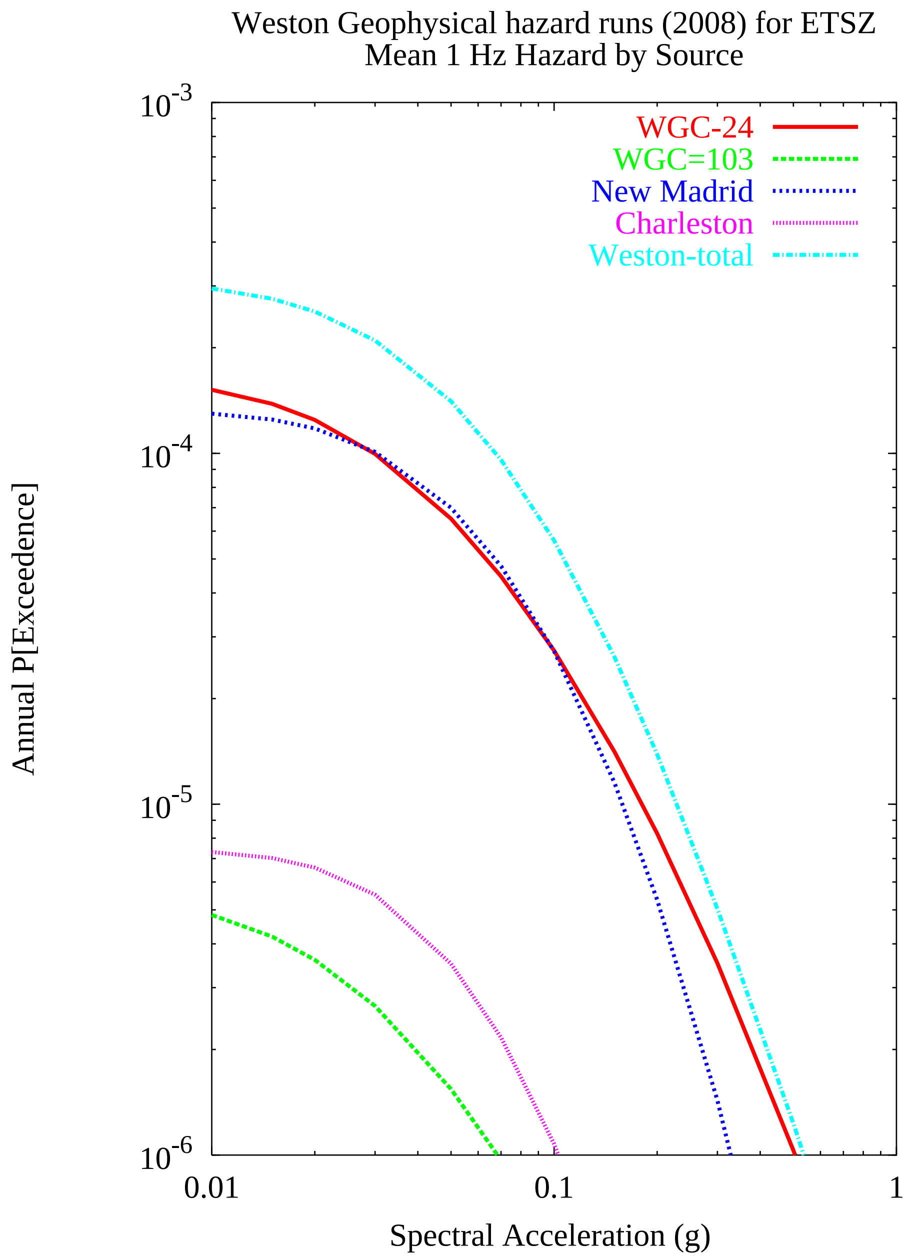


**Figure B9: Weston 1 Hz hazard**

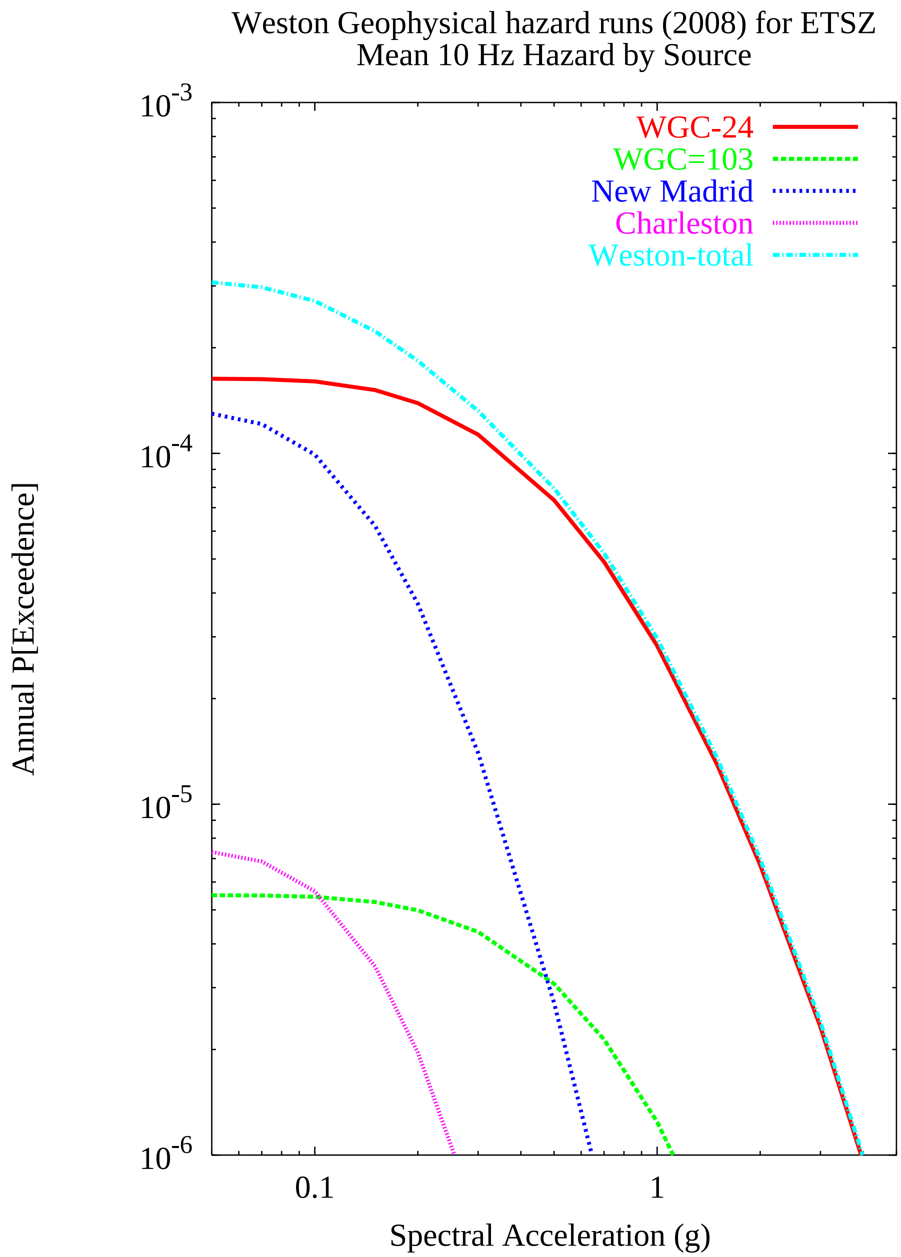


**Figure B10: Weston 10 Hz hazard**

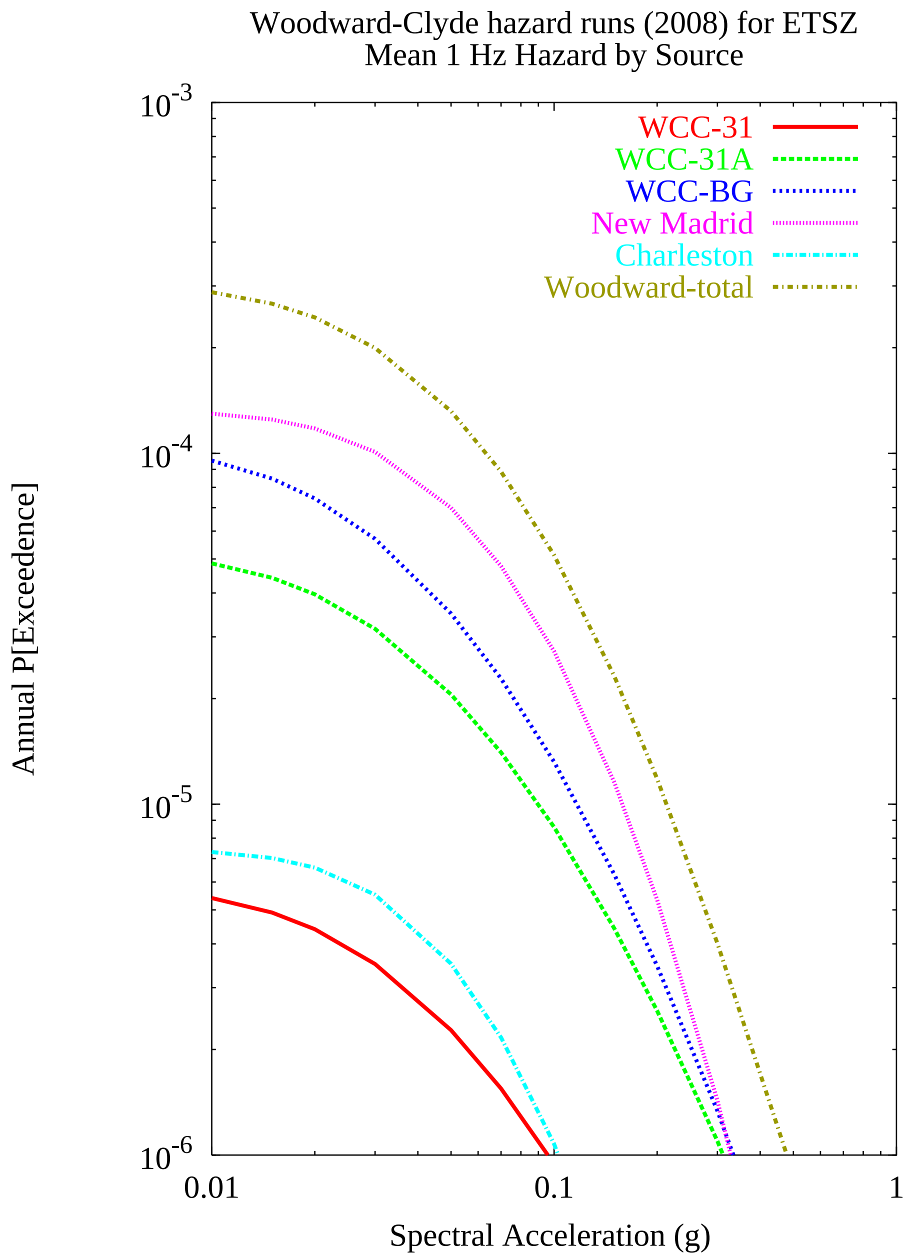


**Figure B11: Woodward-Clyde 1 Hz hazard**

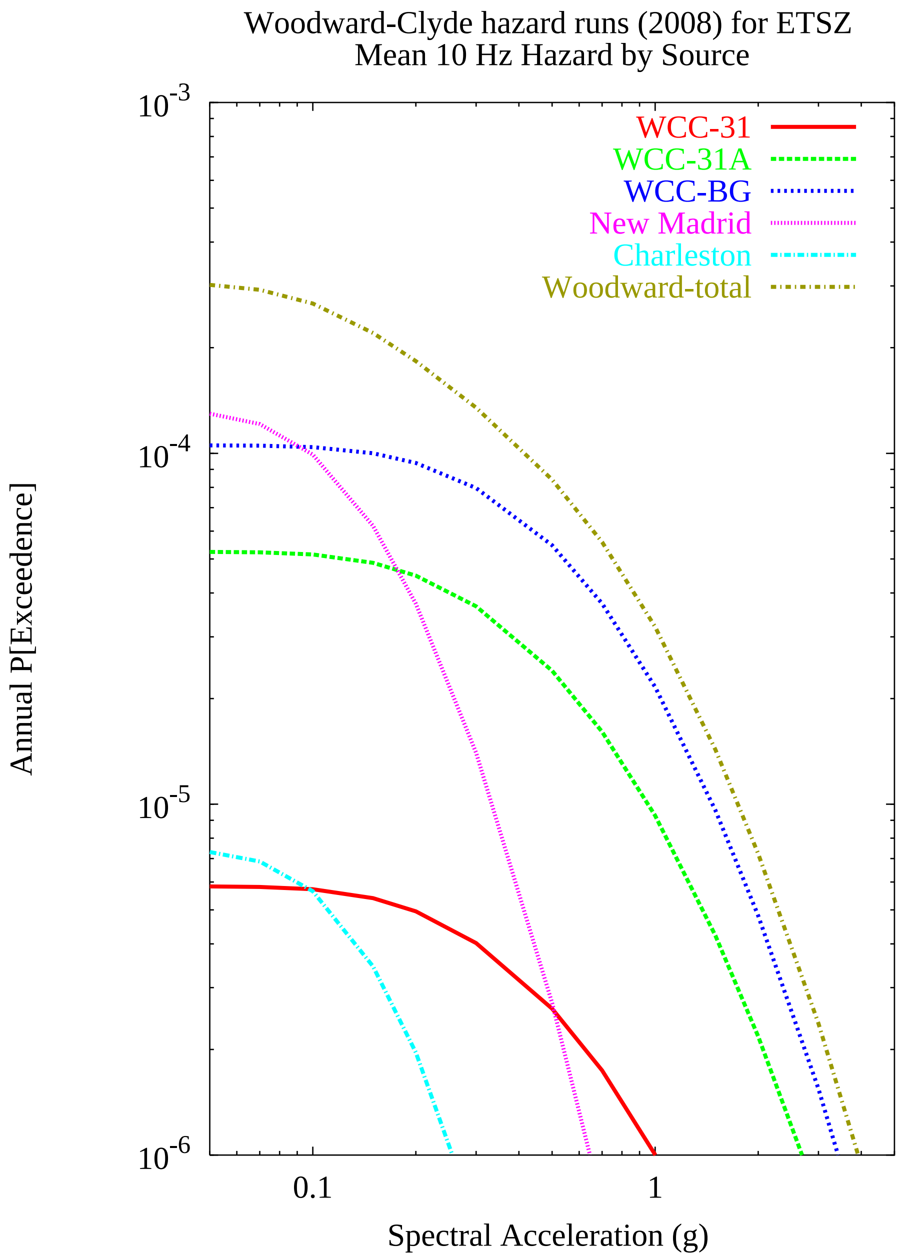


**Figure B12: Woodward-Clyde 10 Hz hazard**